P-06-209

Forsmark site investigation

Mineralogy, geochemistry, porosity and redox capacity of altered rock adjacent to fractures

Björn Sandström, Geology,
Earth Sciences Centre, Göteborg University

Eva-Lena Tullborg, Terralogica AB

September 2006

Svensk Kärnbränslehantering AB
Swedish Nuclear Fuel
and Waste Management Co
Box 5864
SE-102 40 Stockholm Sweden
Tel 08-459 84 00
+46 8 459 84 00
Fax 08-661 57 19
+46 8 661 57 19

ISSN 1651-4416
SKB P-06-209

Forsmark site investigation

Mineralogy, geochemistry, porosity and redox capacity of altered rock adjacent to fractures

Björn Sandström, Geology,
Earth Sciences Centre, Göteborg University

Eva-Lena Tullborg, Terralogica AB

September 2006

Keywords: Wall rock alteration, Redox, Porosity, Geochemistry, Mineralogy, Oxidation.

Abstract

This report presents results from the detailed study of red-stained, altered rock adjacent to fractures at the Forsmark site. The study involves mineralogy, geochemistry, porosity and redox properties of the altered rock and a comparison with fresh rock. The alteration is found in rock adjacent to several fractures in the Forsmark area, and extends normally a few centimetres out from the fractures, although more wide zones are also found. The alteration is typically associated with the precipitation of hydrothermal fracture minerals. The two most abundant rock types within the Forsmark site (medium-grained metagranite to metagranodiorite, rock code 101057 and fine- to medium-grained metagranitoid, rock code 101051) are dealt with in this report.

The major mineralogical changes in the altered rock are the almost complete saussuritization of plagioclase and chloritization of biotite. The red staining in the altered rock is due to sub-microscopic grains of hematite within the saussuritized plagioclase and along the grain boundaries. A small increase in the epidote content can be seen in the altered rock while the K-feldspar is relatively unaffected.

Most chemical elements have been relatively immobile during the hydrothermal alteration, although redistribution of many elements on the micro-scale has occurred which can be seen in the co-existing minerals. The main trends are an increase in K, Na and LOI (Lost on Ignition), while Ca and Fe decrease in the altered rock. The mobility has been small for most of the trace elements. A small decrease in Sr can be seen which is associated with the decrease in Ca, due to the breakdown of plagioclase. No mobility of U and Th has been shown except for one altered sample which has been enriched in Th. The REE content does not differ significantly between the fresh and altered rock.

The connected porosity increases in the altered rock and is mainly due to micro-fractures and an increase in inter-granular porosity due to chloritization of biotite. The saussuritized plagioclase has an increased intra-granular porosity, although this is probably not seen in the porosity data, since most of these pores are not connected.

The redox capacity of the altered rock is slightly lower than in the fresh rock although the difference is small. The mean total oxidation factor increases from 0.20 in the fresh rock to 0.28 in the altered rock, showing that most of the iron in the altered rock, is still in the Fe^{2+} oxidation state.

Sammanfattning

Denna rapport innehåller resultaten från en detaljerad undersökning av rödfärgat omvandlat berg kring sprickor i Forsmark. Studien behandlar mineralogi, geokemi, porositet och redox-egenskaper hos det omvandlade berget och en jämförelse med det oomvandlade berget. Omvandlingen finns i anslutning till flera sprickor i Forsmarksområdet, och omfattar oftast några få centimeter runt sprickorna, även om mer omfattande zoner med omvandling finns. Omvandlingen är ofta associerad med utfällningar av hydrotermala sprickmineral. De två mest förekommande bergarterna i Forsmarksområdet (medelkornig metagranit till metagranodiorit, bergartskod 101057 och fin- till medelkornig metagranitoid, bergartskod 101051) behandlas i denna rapport.

Den huvudsakliga mineralogiska förändringen i det omvandlade berget är en näst intill total saussuritisering av plagioklas och kloritisering av biotit. Den röda färgen hos det omvandlade berget beror på små mikrokorn av hämatit i den omvandlade plagioklasen och längs korn-gränser. Kalifältspaten är relativt oomvandlad, medan en liten ökning av epidot-innehållet kan påvisas i det omvandlade berget.

De flesta ämnen har varit relativt immobila under den hydrotermala omvandlingen, även om en omfördelning på den mikroskopiska skalan har ägt rum vilket kan ses mineralogiskt. Den huvudsakliga förändringen i geokemi är en ökning av K, Na och LOI (Lost on ignition) medan Ca och Fe har minskat i det omvandlade berget. Mobiliteten hos spårämnena i bergarterna har varit låg. Dock kan en liten minskning av Sr ses vilken är associerad med minskningen av Ca på grund av nedbrytningen av plagioklas. Ingen mobilitet hos U eller Th har kunnat påvisas förutom i ett prov som har blivit anrikat på Th. REE innehållet har inte förändrats i det omvandlade berget.

Den effektiva porositeten har ökat i det omvandlade berget på grund av en ökad frekvens av mikrosprickor och en ökad porositet längs den kloritiserade biotitens korngränser. Den saussuri-tiserade plagioklasen har en ökad porositet i liten skala innuti de omvandlade mineralkornen, men detta syns antagligen inte i porositetsmätningarna, då dessa porer inte står är i förbindelse med varandra.

Redox-kapaciteten hos det omvandlade berget är något lägre än hos icke omvandlat berg, men skillnaden är liten. Den totala oxidationsfaktorn ökar från 0,20 i det oomvandlade berget till 0,28 i det omvandlade berget vilket visar att järn främst förekommer som Fe^{2+} även i det omvandlade berget.

Contents

1 Introduction

This document reports the results gained by the comparative study of the mineralogy, geochemistry, porosity and redox conditions in rock adjacent to fractures, which is one of the activities performed within the site investigation at Forsmark. The work was carried out in accordance with activity plan AP PF 400-05-76. In Table 1-1 controlling documents for performing this activity are listed. Both activity plan and method descriptions are SKB's internal controlling documents.

Zones of altered, red-coloured wall rock are found adjacent to several fractures in the Forsmark area (Figure 1-1). The altered zone extends a few centimetres from the fractures, although wider zones are found. The latter are often associated with penetrative networks of minor fractures. The altered rock is briefly described by /Sandström et al. 2004, Sandström and Tullborg 2005/ and is found adjacent to fractures sealed with hydrothermal minerals, including epidote, adularia, prehnite, laumontite, calcite and hematite. The red colour in the altered rock is due to sub-microscopic grains of hematite, mainly in the plagioclase. The altered wall rock is also found adjacent to many open fractures due to fracturing and later reactivation of older hydrothermal fracture fillings or dissolution of fracture fillings.

Since the altered rock makes up a large portion of the interface between rock and the water conductive fractures, the understanding of the properties of this rock is important for e.g. the transport modelling. Furthermore, it is important to get knowledge about how large the remaining redox capacity of the altered rock is.

Table 1-1. Controlling documents for the performance of the activity.

Activity plan	**Number**	**Version**
Undersökning av bergets redox-kapacitet i ansluting till sprickor	AP PF 400-05-76	1.0
Method descriptions	**Number**	**Version**
Metodbeskrivning för bergartsanalyser	SKB MD 160.001	1.0
Metodbeskrivning för sprickmineralogiska undersökningar	SKB MD 144.001	1.0

Figure 1-1. *Red-coloured altered wall rock adjacent to calcite- and chlorite-coated fracture. The diameter of the drill-core is ~ 5 cm, KFM08A 623.03–623.35 m.*

The results include mineralogy, geochemistry, redox properties (Fe^{3+}/Fe_{tot}) and porosity. Altered and fresh rock samples have been obtained from drill cores from the telescopically drilled boreholes KFM01A, KFM01B, KFM02A, KFM03A, KFM04A, KFM05A, KFM07A, KFM08A, KFM08B and KFM09A. The locations of the boreholes are shown in Figure 1-2. Previously published geochemical data /Petersson et al. 2004, 2005/ of fresh rock have been used as reference data.

Previous studies of red-stained, altered rock similar to that it Forsmark have been carried out at Äspö, Simpevarp and Laxemar /Eliasson 1993, Drake and Tullborg 2006ab/. All theses studies conclude that the red-staining is due to fine-grained hematite and/or Fe-oxyhydroxide within altered plagioclase, along grain boundaries and in micro fractures. The main mineralogical changes are the saussuritization of plagioclase, chloritization of biotite and hematization of magnetite in the altered rock. The same studies show that the main geochemical changes are an increase in K, Na, LOI and Rb in the altered rock while Ca and Sr decreases and REEs and most other trace elements remain relatively constant during the alteration.

The two major rock types, considered in this report, occupy ~ 94% of the rock volume inside the candidate area. Of these, the medium-grained meta-granitic to meta-granodiorite (rock code 101057) occupies ~ 84% of the rock volume and the fine- to medium-grained metagranitoid (rock code 101051) occupies ~ 10% /SKB 2006/.

All results are stored in the SKB data base SICADA, and are traceable by the activity plan number.

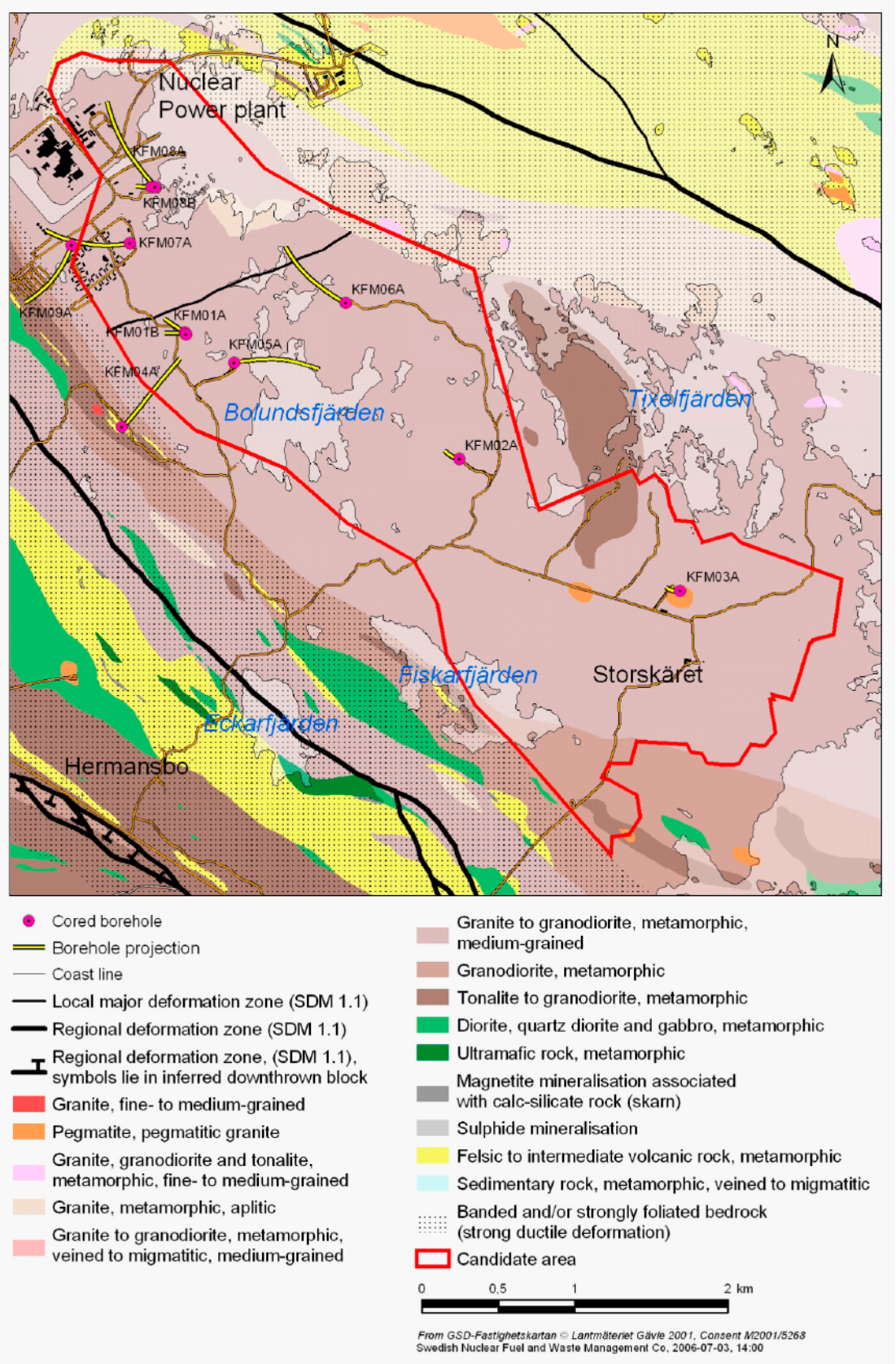

Figure 1-2. *Bedrock geology of the Forsmark site investigation area with projections of the boreholes dealt with in this report. /SKB GIS database 2006/.*

2 Objective and scope

The aim with the present study is to:

- Describe the changes in mineralogy, geochemistry, porosity and redox capacity between the fresh and altered rock.
- Provide data of the redox capacity for both fresh and altered rock.
- Provide geochemical and redox capacity data of fracture networks sealed with epidote and laumontite.

Table 2-1. Analyses carried out on samples selected for this study. xx = two sub-samples have been analysed from the same drill core sample.

Borehole	Secup	Seclow	Altera-tion	Rock type	Point counting	SEM-EDS	Whole rock geochemistry	S (ppm)	Möss-bauer	Porosity
KFM01A	103.31	103.46	No	101057						x
KFM01A	312.50	312.92	No	101057						x
KFM01A	477.30	477.30	No	101057	x	x				
KFM01A	521.10	521.40	No	101051	x			x	x	
KFM01A	704.00	704.40	No	101057						x
KFM01A	521.27	521.27	No	101051	x					
KFM01B	36.66	37.15	Yes	101057			x	x	x	x
KFM01B	37.41	37.80	Yes	101057						x
KFM01B	41.89	42.05	Yes	101057			x	x		
KFM01B	52.01	52.34	Yes	Epidote network			x	x	x	
KFM01B	397.41	394.76	No	101057	x	x	x	x		x
KFM01B	416.50	416.77	Yes	101057			x	x	x	x
KFM01B	434.33	434.70	Yes	Laumontite network			x	x	x	
KFM02A	350.50	350.60	No	101057						x
KFM02A	483.64	483.97	Yes	101057			x		x	x
KFM02A	495.64	495.88	Yes	101057	x	x	x	x	x	x
KFM02A	500.35	500.55	Yes	101051						x
KFM02A	502.64	502.85	Yes	101051	x	x	x	x	x	
KFM02A	503.78	503.97	Yes	101051	x		x	x	x	x
KFM02A	506.80	507.10	Yes	101057	x	x	x		x	x
KFM02A	712.05	712.25	No	101057				x	x	
KFM02A	712.45	712.48	No	101057	x	x				
KFM02A	915.80	915.90	No	101051			x			
KFM02A	949.87	949.90	No	101057	x	x				
KFM02A	949.90	950.10	No	101057				x	x	
KFM02A	953.45	953.48	No	101057	x	x				
KFM02A	953.68	953.78	No	101057						x
KFM03A	311.33	311.43	No	101051			x			
KFM04A	694.65	694.80	No	101057						x
KFM07A	183.13	183.41	Both	101057	x	x	xx	xx	xx	
KFM08B	91.36	91.58	Both	101057	xx	x	xx	xx	xx	
KFM08A	623.02	623.35	Both	101057	x	x	xx	x	xx	
KFM09A	150.67	150.83	No	101051				x	x	x
KFM09A	172.82	172.97	No	101051				x	x	x

3 Equipment

3.1 Description of equipment/interpretation tools

The following equipment was used for the study.

- Rock saw.
- Swing mill.
- Digital camera.
- Scanner.
- Petrographic microscope (Leica DMRXP).
- Digital microscope camera (Leica DFC 280).
- Scanning electron microscope (HITACHI S-3400N).
- EDS-detector (INCADryCool).
- Point counting equipment.

The equipment listed above is located at the Earth Sciences Centre, Göteborg University, Sweden. For instruments used for Mössbauer spectroscopy, porosity measurements and analyses of whole rock chemistry and sulphur, see Section 4.4.

4 Execution

4.1 General

Samples from drill cores KFM01A, KFM01B, KFM02A, KFM03A, KFM04A, KFM07A, KFM08A, KFM08B and KFM09A of both altered (mapped as oxidized in Boremap) and fresh rock have been selected for analysis. Totally 13 samples of altered rock and 10 samples of unaltered rock were selected from the drill cores. In addition, rock powder and thin sections of fresh rock were provided by SKB. Totally 15 thin sections were analysed, 21 samples were crushed and ground for whole rock geochemical analyses, 19 samples for analysis of sulphur, 18 samples were selected for Mössbauer analysis and 17 for porosity and density measurements.

Quantitative optical microscopy of thin sections provides modal mineralogical composition while studies with SEM-EDS provide a description of e.g. the distribution of Fe-oxides on the sub micro-scale, as well as the chemical composition of individual minerals.

Geochemical analyses on whole rock samples have been carried out using ICP-AES and ICP-MS in order to distinguish which elements have been mobile/immobile during the alteration. Altered samples were compared to reference data of fresh rock from /Petersson et al. 2004, 2005/.

The connected porosity has been measured, using water saturation technique on both altered and unaltered drill core sample. Although porosity data of the unaltered rock are available in e.g. /SKB 2005/, the complexity of porosity measurements, /e.g. Drake et al. 2006, Tullborg and Larson 2006/ called for synchronous analyses of both altered and unaltered rock in order to obtain comparable results.

The redox properties of altered and unaltered rock were carried out by Mössbauer spectrometry technique, which gives the oxidation factor of the rock (Fe^{3+}/Fe_{tot}).

The geochemistry and redox capacity of one epidote and one laumontite sealed fracture network were also analysed.

The method descriptions used are SKB MD 160.001 and SKB MD 144.001 (SKB internal documents).

4.2 Preparations

Drill core samples were documented using a digital camera before any processing.

Where enough material was available, the drill core was sawed into one 5 cm long section for porosity measurements, one thin disc was sawed for thin section preparation and one ~ 10 cm long section for chemical and Mössbauer analysis.

Fracture fillings were removed by rock saw, before the samples were crushed with a rock hammer and ground in a swing mill for chemical and Mössbauer analyses. In some altered samples, micro-fractures were impossible to avoid but since they are characteristic for the altered wall rock, their presence is not considered a problem.

Polished thin-sections with a thickness of 30 μm were prepared at Earth Sciences Centre, Göteborg University.

4.3 Execution of field work

Altered rock samples were selected from red-coloured parts of the drill cores. The sampled drill core depths were correlated with WellCad data from SICADA, to confirm that the samples were mapped as altered (oxidized) during the drill core mapping.

Since the alteration of the wall rock often is limited to a few centimetres around the fractures, larger altered zones have preferably been sampled to get material enough, in order to carry out all the analyses required from a single sample. Since apparently fresh rock adjacent to altered rock often is altered, even though this can not be detected macroscopically, the comparison has been made based on mean values of fresh rock far away from fractures and apparently altered rock.

As unaltered reference rock samples were preferably selected from drill core sections where chemical data already existed /Petersson et al. 2004, 2005/, these samples were provided by SKB as rock powder, together with corresponding thin sections for further analyses (Mössbauer, sulphur and detailed mineralogy).

4.4 Analytical work

The quantitative mineralogical analyses were carried out by point counting, i.e. by determining the mineralogy at 1,000 evenly spaced points in each thin section using a petrographic microscope. Although modal composition of the fresh rock is available in /Petersson et al. 2004, 2005/ the resolution of this data (500 points per thin section) was not high enough for the detection of variation in the amount of accessory minerals, why both fresh and altered rock were analyses for modal composition within the scope for this report. Point counting is also somewhat subjective and in order to get comparable results it was an advantage that the same person carried out point-counting on both fresh and altered rock.

The SEM/EDS analyses were carried out on a Hitachi S-3400N equipped with an INCADryCool EDS detector.

Chemical analyses were carried out at Acme Analytical Laboratories Ltd in Vancouver, Canada. The oxides SiO_2, Al_2O_3, Fe_2O_3, MgO, CaO, Na_2O, K_2O, TiO_2, P_2O_5 and MnO were analysed with ICP-AES, C and S by the Leco method and trace elements (Mo, Cu, Pb, Zn, Ni, As, Cd, Sb, Bi, Ag, Au ,Hg, Tl, Se, Ba, Be, Co, Cs, Ga, Hf, Nb, Rb, Sn, Sr, Ta, Th ,U, V, W, Zr, Y and REE) with ICP-MS. The method is described in /Stephens et al. 2003/.

Mössbauer analyses were carried out by Prof. Hans Annersten, Uppsala University, according to the method described in /Drake and Tullborg 2006b/.

The connected porosity measurements were carried out by the water saturation technique at SP (Swedish National Testing and Research Institute) according to the European standard EN 1936 on 5 cm long drill cores (5 cm in diameter).

Analyses of S with ppm resolution were carried out by Analytica AB in Luleå, Sweden. The method is described in /Drake and Tullborg 2006b/.

4.5 Nonconformities

The activity has been performed according to the activity plan without any nonconformities.

5 Results

The original results are stored in the primary data bases (SICADA). The data is traceable in SICADA by the Activity Plan number (AP PF 400-05-76).

The data is also presented in tables and as appendices in this report. The appendices are:

Appendix 1 Sample description

Appendix 2 Whole rock geochemistry

Appendix 3 SEM-EDS analyses of biotite and chlorite

Appendix 4 Modal analyses of thin sections

5.1 Mineralogy

The main differences between fresh and altered rock is the saussuritization of plagioclase and the replacement of biotite with chlorite. The epidote content is also somewhat higher in the altered rock although the variation is large. The content of opaque minerals is less than 1 vol% in all analysed samples (mean 0.2 vol%), both fresh and altered (Figure 5-1 and 5-2).

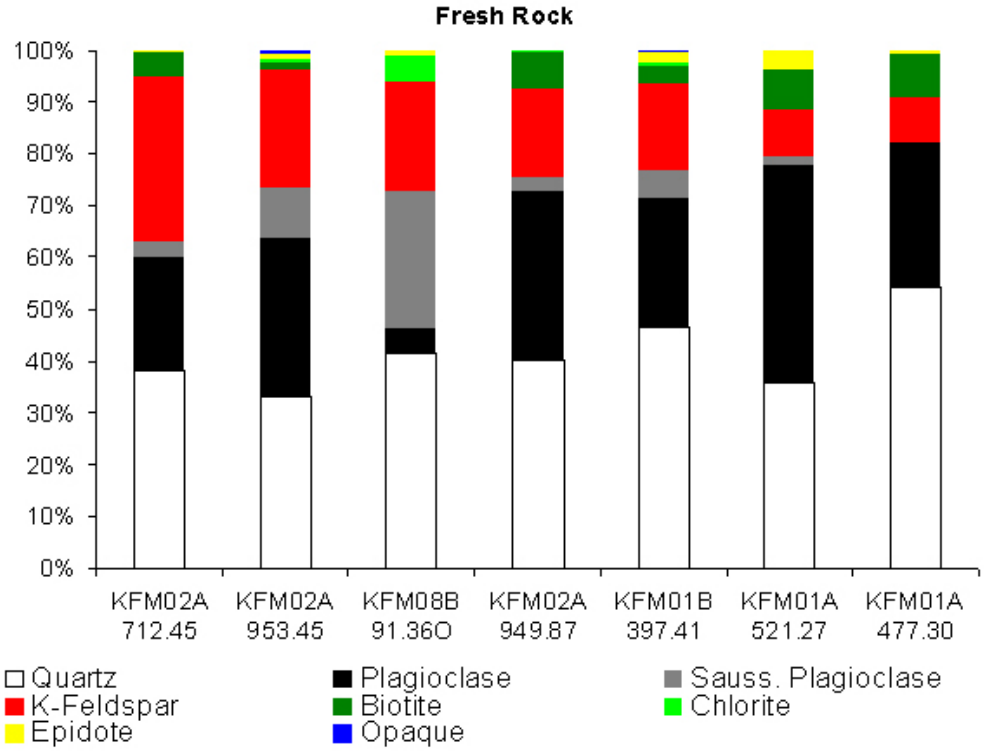

Figure 5-1. *Modal mineralogy of apparently fresh rock based on point counting (1,000 points).*

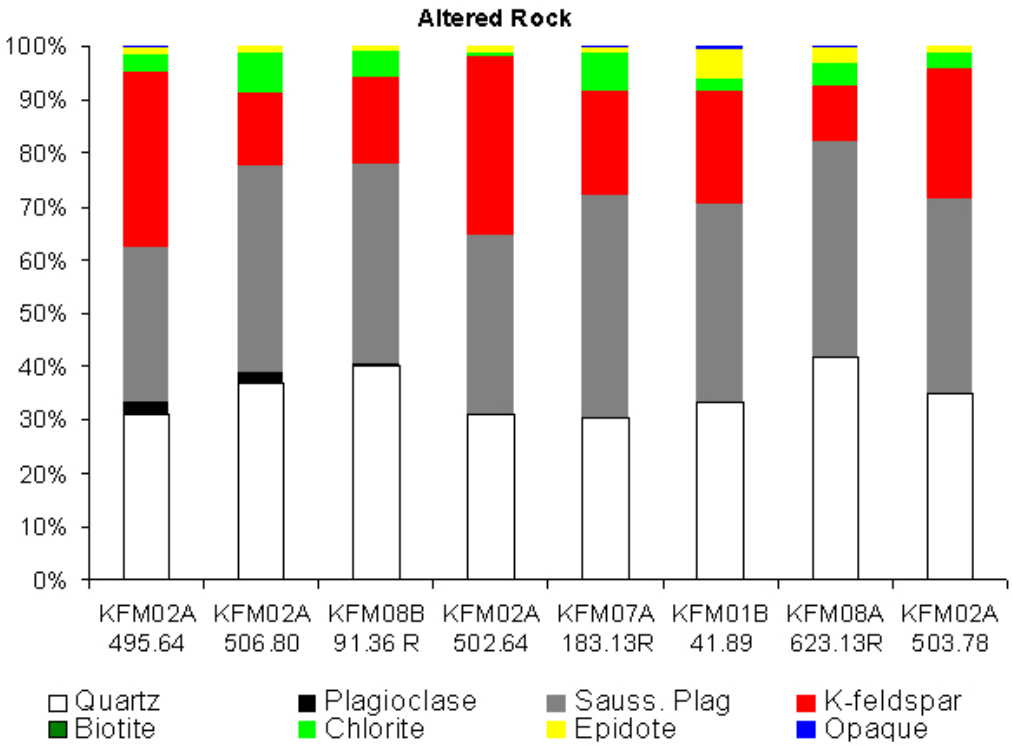

Figure 5-2. *Modal mineralogy of altered rock based on point counting (1,000 points).*

Sections of the drill-cores with adjacent apparently fresh and red-coloured altered rock show that the alteration is more widespread than the red-colouring indicates. Rock adjacent to the altered red-coloured zone that macroscopically appears unaltered often shows completely chloritized biotite and most of the plagioclase has been saussuritized although not as intensely as in the red-coloured rock. This has also been described in altered rock from the Oskarshamn site in southern Sweden /Drake and Tullborg 2006ab/ and can be seen in sample KFM08B 91.36O in Figure 5-1.

Plagioclase

The main difference between the fresh and altered rock is the almost complete saussuritization of plagioclase; the plagioclase of oligoclase composition ($An_{\sim 16}$) has been replaced by a mineral assemblage composed of albite ($Ab_{\sim 05}$) with small adularia crystals together with epidote, sericite, hematite and small amounts of calcite. The sub-microscopic grains of hematite occur both within grains and along grain boundaries of the saussuritized plagioclase, giving the plagioclase the red colour responsible for the red colour of the altered rock. Small hematite grains are also concentrated along the crystal boundaries (Figure 5-3). In partly altered crystals, the alteration can be seen to follow cleavage planes in the plagioclase and it can also be seen that the intra-granular porosity increases in the altered plagioclase with pores from less than a micron to a few microns across (Figure 5-4). Although the saussuritization often is almost complete, the original albitic twinning can still be seen in many of the altered grains (Figure 5-5).

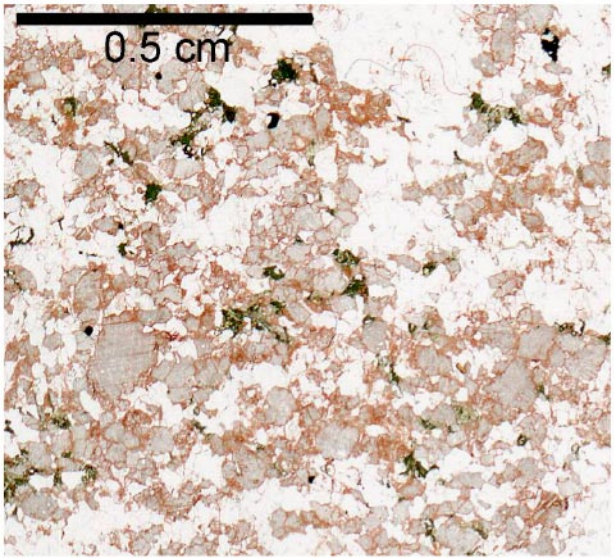

Figure 5-3. *Scanned thin section of altered rock showing how the red-staining is concentrated within and along grain boundaries of the altered plagioclases which are the cloudy grains in the figure, KFM08A 623.13–623.35 m.*

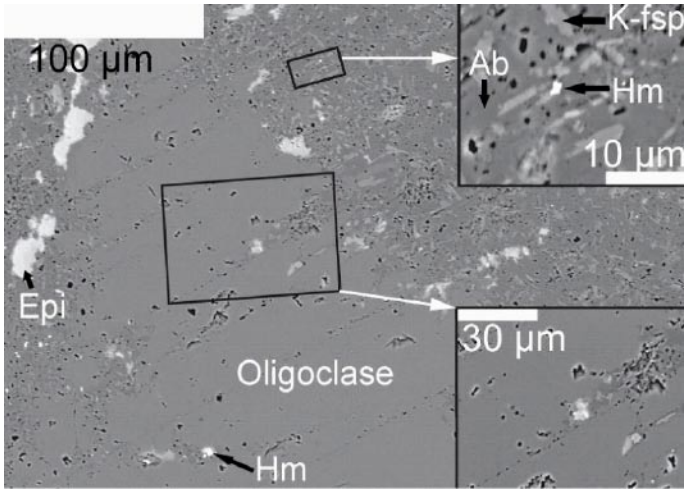

Figure 5-4. *Backscattered electron image of plagioclase with oligoclase composition ($An_{\sim 16}$) partly replaced by albite ($An_{\sim 05}$) with small K-feldspar crystals (K-fsp), epidote (Epi) and sub-microscopic grains of hematite (Hm). The porosity of the albite is higher and the alteration can be seen to follow the cleavage planes in the oligoclase, KFM05A 692.00B.*

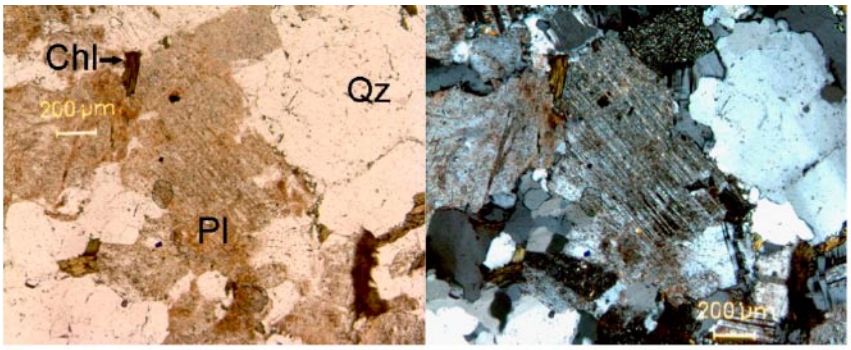

Figure 5-5. *Photomicrograph of saussuritized plagioclase in altered rock (left) and with crossed polars where the original albitic twinning has been preserved (right),Chl = chlorite, Qz = quartz and Pl = plagioclase, KFM08A 90.63R.*

K-feldspar

While the plagioclase in the altered rock is highly saussuritized, the primary K-feldspar (microcline) has been preserved during the alteration and its characteristic cross-hatched twin pattern is identical with that shown in K-feldspar in apparently unaltered rock samples (Figure 5-6). Only in a few samples have faint sericitization of K-feldspar been observed. The K-feldspar's resistance against alteration has also been recognised in altered granitic rock at the Oskarshamn site in southern Sweden /Drake and Tullborg 2006ab/.

Secondary low-temperature K-feldspar (adularia) has crystallized as small crystals within the saussuritized plagioclase (Figure 5-4).

Biotite – Chlorite

The biotite has been completely chloritized in the altered rock and in the most intensely altered samples replaced by clay mineral (most likely corrensite). The chlorite contains lenses of titanite, adularia, prehnite and pumpellyite and often quartz and accessory minerals like zircon and apatite (Figure 5-7).

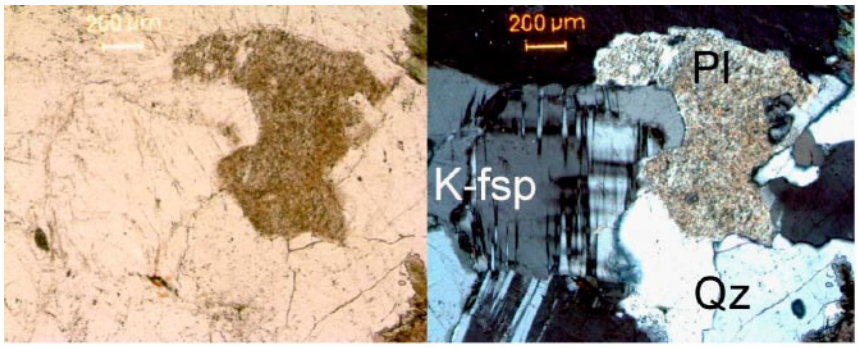

Figure 5-6. *Photomicrograph of unaltered K-feldspar (K-fsp) next to highly saussuritized plagioclase (Pl) and quartz (Qz). Plain polarized light (left) and crossed polars (right), KFM02A 500.32 m.*

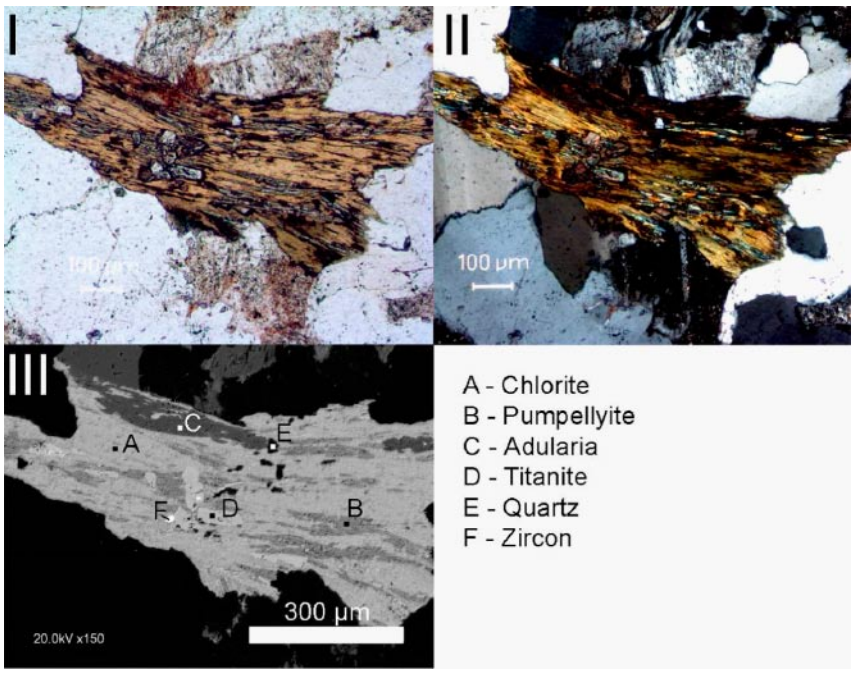

Figure 5-7. *Chlorite pseudomorph after biotite with lenses of adularia and pumpellyite together with titanite, quartz and zircon. I) Photomicrograph, II) Crossed polars, III). Backscattered electron image, KFM08B 91.36–91.58 m.*

The biotite in the fresh rock has a Fe_{total} content given as FeO of ~ 24–28 wt% while the chlorite in the altered rock has a higher FeO content of ~ 31–40 wt% (based on SEM-EDS analyses, Appendix 3). The MgO content varies highly in both the biotite and chlorite between ~ 5–10 wt% but there is no difference in MgO content between biotite and chlorite (Figure 5-8). A correlation can be seen between the MgO content in biotite and in the whole rock chemistry (Figure 5-9). No correlation between the Fe content in biotite and whole rock can be seen (Figure 5-10). A possible source for the Fe that has been incorporated into the chlorite is the Fe made available during the alteration of magnetite into hematite during the alteration. Increased Fe-content in pseudomorphic chlorite compared to parental biotite has previously been described by e.g. /Parneix et al. 1985/ and /Drake and Tullborg 2006ab/ although decrease in Fe during chloritization also occurs, showing that the biotite composition does not strictly control the composition of the secondary chlorite /Parneix et al. 1985/. During the breakdown of biotite, the potassium is incorporated in newly formed lenses of adularia within the chlorite while titanium is incorporated in titanite lenses. The presence of prehnite or pumpellyite as lenses in the chlorite (as well as titanite) reveals transport of calcium into the crystallization site during the chloritization of biotite and indicates that the saussuritization of plagioclase and chloritization of biotite were coeval. The chloritization extends further away from the fractures than can be seen from the red-colouring of the wall rock.

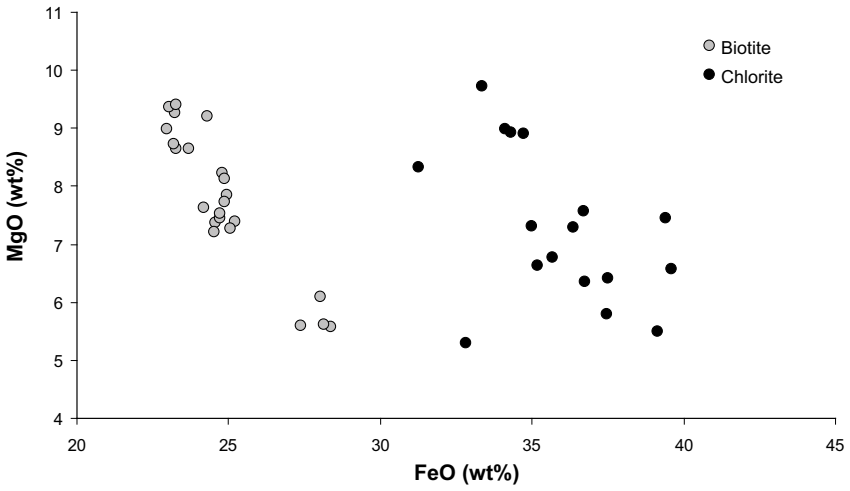

Figure 5-8. *$Fe_{(total)}$ given as FeO versus MgO in biotite and chlorite.*

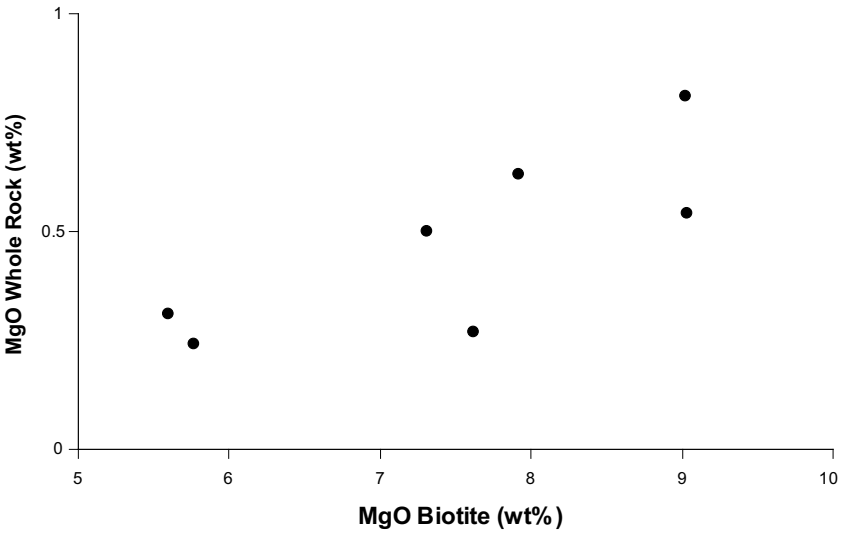

Figure 5-9. *MgO in biotite versus MgO in whole rock.*

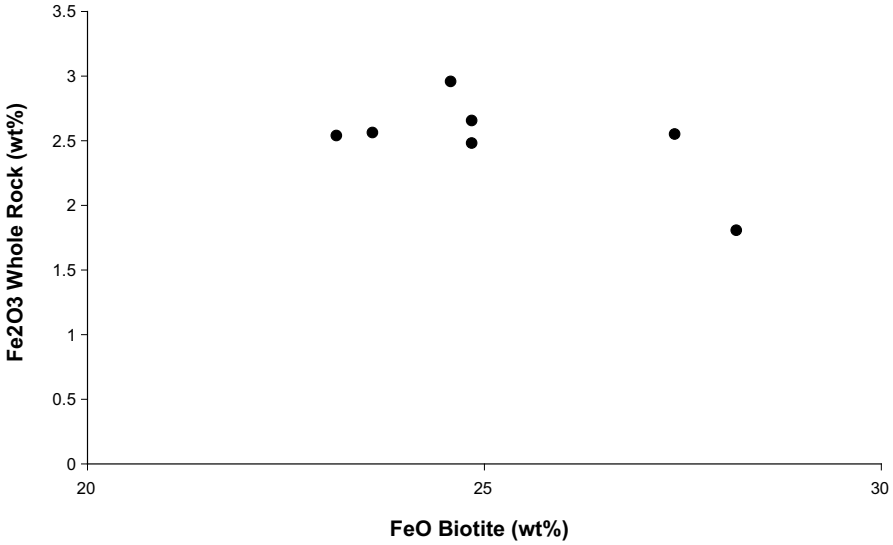

Figure 5-10. *$Fe_{(total)}$ given as FeO in biotite versus $Fe_{(total)}$ given as Fe_2O_3 in whole rock.*

Epidote

Epidote is found in different amounts in all samples, a small increase in the epidote content can be seen in altered samples compared to fresh rock (Appendix 4). The amount of epidote varies between 0.2 and 3.6 vol% in the fresh samples and between 0.6 and 5.7 vol% in the altered samples. Epidote contains only Fe^{3+} and has a Fe_2O_3 content of ~ 9–17 wt% based on SEM-EDS analyses /Sandström et al. 2004, Sandström and Tullborg 2005/.

Magnetite and hematite

Mössbauer analyses show that magnetite and hematite occur in both fresh and altered rock and are the most common opaque minerals. From microscopic studies, it can be seen that unaltered magnetite crystals occur in the fresh rock (Figure 5-11) while the magnetite crystals in altered rock often are partly replaced by hematite (Figure 5-12). In the altered rock, hematite also occurs as sub-microscopic grains in, and along the grains boundaries of saussuritized plagioclase. Magnetite is the most common opaque mineral in the fresh samples. All together, opaque minerals make up less than 1 vol% in both fresh and altered rock, although in the altered rock the sub-microscopic grains of hematite are not included in this number since they are only detectable in the electron microscope.

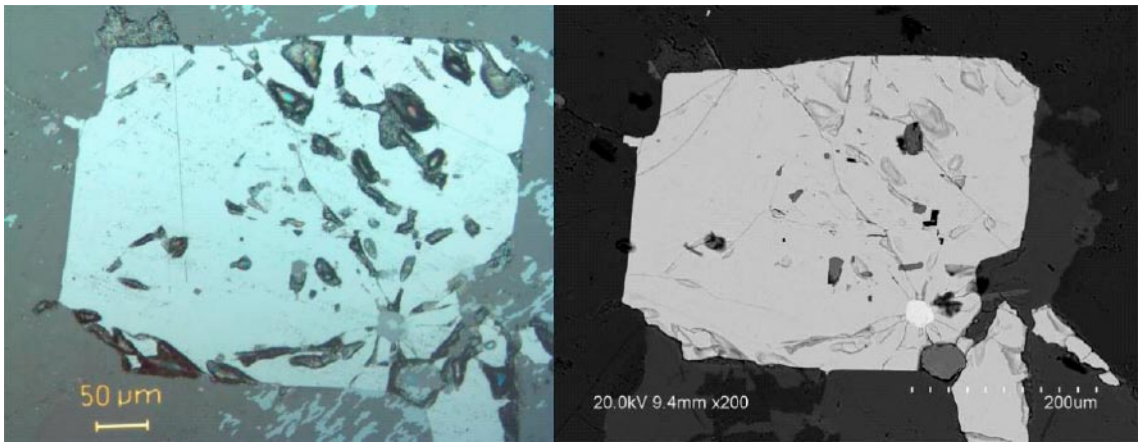

Figure 5-11. *Photomicrograph in reflected light of magnetite in fresh rock (left), and backscattered electron image of the same crystal (right). The small white grain is zircon, KFM02A 953.45 m.*

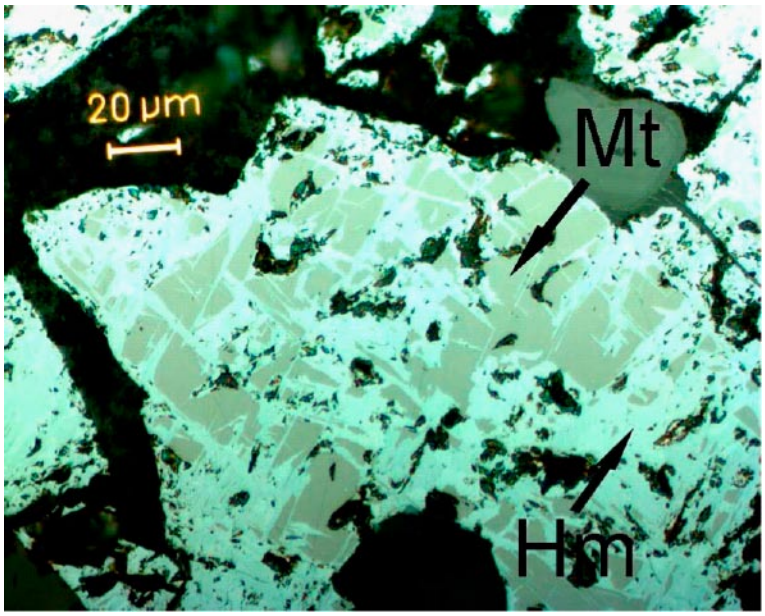

Figure 5-12. *Photomicrograph in reflected light of magnetite grain partly replaced by hematite in altered rock, KFM01B 36.66 m.*

Pyrite

Pyrite occurs in small amounts in both fresh and altered rock, the presence of pyrite in altered rock samples (Figure 5-13) indicate that the oxidation of the rock was quite limited during the hydrothermal alteration.

5.2 Whole rock geochemistry

For the comparative study, data from /Petersson et al. 2004, 2005/ of fresh rock has been used as reference.

Mass change normalization

During metasomatism it is common with gain or loss of mass and/or changes in volume. Thus, when the elemental concentrations of fresh and altered rock are compared, the results can be deceptive if they are not normalized. A method for mass-balance analyse is described by /Gresen 1967/. This method is based on the assumption that some elements are immobile and therefore

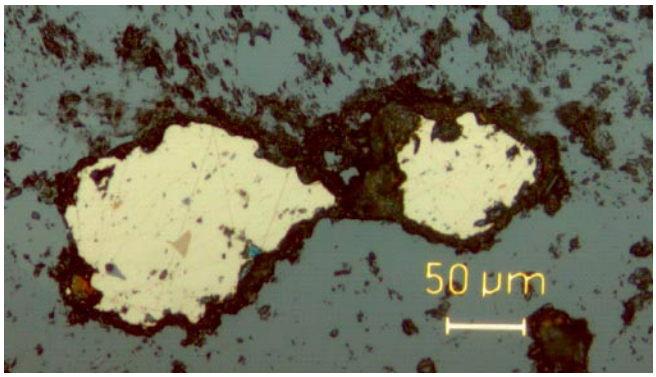

Figure 5-13. *Photomicrograph in reflected light of pyrite surrounded by chlorite in altered rock, KFM02A 506.80 m.*

conserved during the metasomatism. The ratio of mobile elements in the fresh and altered rock is then compared to the ratio of the immobile elements in order to calculate the mass or volume loss during the metasomatism. An isocon diagram can be used to graphically solve this problem /Grant 1986/; the geochemical composition of the fresh rock is plotted versus the altered rock (Figure 5-14). In the isocon diagram the immobile elements will define a straight line through the origin – an isocon. The slope of the isocon defines the ratio of equivalent masses (M^0/M^A) in the fresh rock (M^0) and in the altered wall rock (M^A). Elements above this line have been enriched relative to the fresh rock while elements below the line have been depleted. The slope of the isocon yields the mass change of the altered rock; a slope greater than one indicates a mass loss while a slope less than one indicates a mass gain. The deviation of data points from the isocon gives the change in concentration. The normalized normative change in element concentration (ΔC) can then be calculated from $\Delta C/C^0 = (M^A/M^0)(C^A/C^0)–1$.

Aluminium is used as an immobile element in the isocon diagram (Figure 5-14) because of its often conservative behaviour during metasomatism e.g. /Baker 1985, Grant 1986/ and the low standard deviation. Other elements usually considered immobile have been disregarded either due to high standard deviations due to low concentrations and/or inhomogeneity (e.g. Ta and Y).

The slope of the isocon (M^A/M^0), in Figure 5-14 is 1.0376 (based on Al as immobile element) which yields $M^0/M^A = 0.964$, equivalent to a mass loss of 3.6%.

If instead the mass change obtained from the density measurements (mean mass decreases 2.4%, see Section 5.3) is used to normalize, the following equation can be used to normalize the element concentrations: $\Delta C/C^0 = (\rho^0/\rho^A)(C^A/C^0)–1$, where ρ^0 is the density of the fresh rock and ρ^A the density of the altered rock. A straight line with a slope defined by the measured densities (ρ^0/ρ^A) can be drawn in the isocon diagram (grey line in Figure 5-14) The difference between the two lines is not so large, but the normalization based on the measured mass change is preferred since the abundance of Al-silicates in fractures coeval to the wall rock alteration clearly show that aluminium was to some extent mobile during this period. The results from the two different normalizations are shown together with the un-normalized for some selected elements in Figure 5-15.

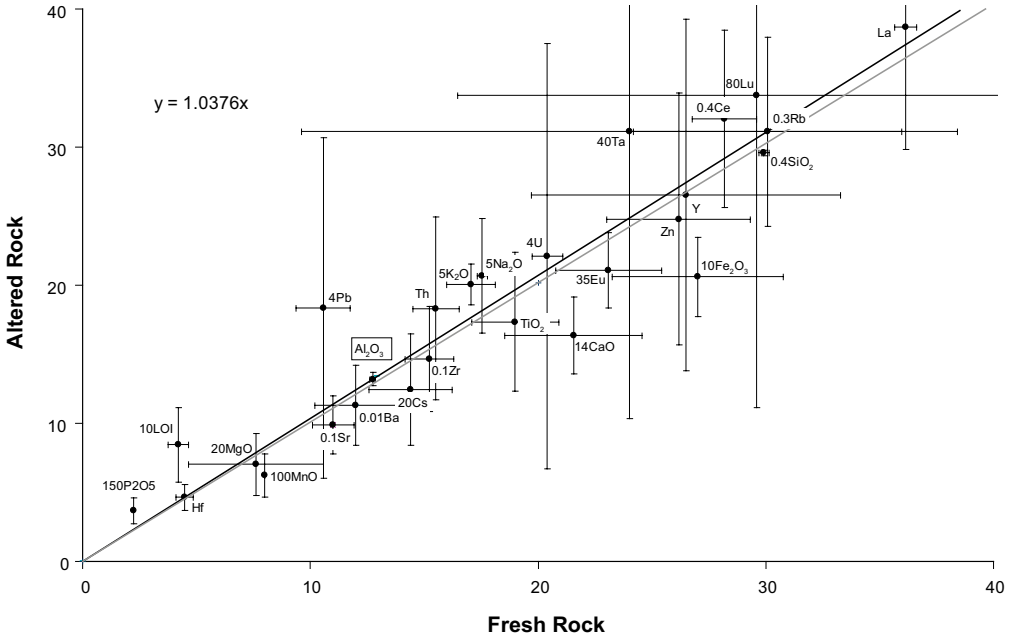

Figure 5-14. *Isocon diagram for the alteration of granitic to granodioritic rock to altered rock. Elements above the line have been enriched in the oxidized rock compared to the fresh rock while the elements below the line have been depleted. The grey line represents equivalent masses based on the measured densities. Major elements and LOI (lost on ignition) are plotted as wt% and trace elements as ppm. Error bars are 1σ standard deviations for the altered samples.*

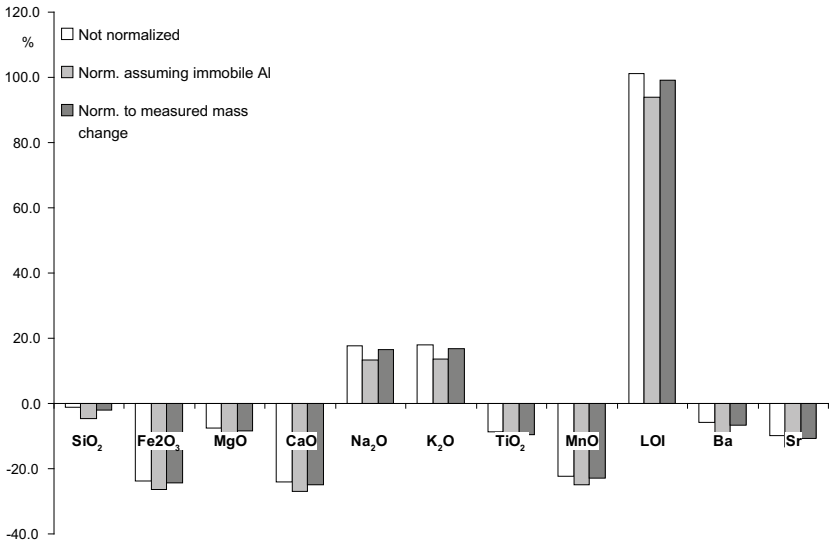

Figure 5-15. *Plot of mean relative change for selected element concentrations in the altered rock compared to fresh rock. The white bar is not normalized for mass change, the light grey bar is normalized assuming immobile Al and the dark grey bar is normalized based on the measured mass change.*

Medium-grained metagranite to metagranodiorite – rock code 101057

The mean geochemistry of fresh and altered rock is presented in Table 5-2.

Si, Al, LOI

The mean SiO_2 and Al_2O_3 contents are relatively unchanged in the altered rock, compared to the fresh rock (Figure 5-16). A trend can however be seen when SiO_2 is plotted against Al_2O_3 for the individual samples where SiO_2 decreases in the altered rock and Al_2O_3 increases (Figure 5-17). The mean normalized relative changes are –2.0 and +2.7% respectively (Figure 5-16). The decrease in SiO_2 and increase in Al_2O3 can be explained by the albitization of plagioclase and the chloritization of biotite.

The mean LOI has changed from 0.42 to 0.84 wt% in the altered rock compared to the fresh rock giving a normalized relative change of +99.2% (Figure 5-18). This change is mostly due to the chloritization of biotite but also the saussuritization of plagioclase producing sericite and epidote.

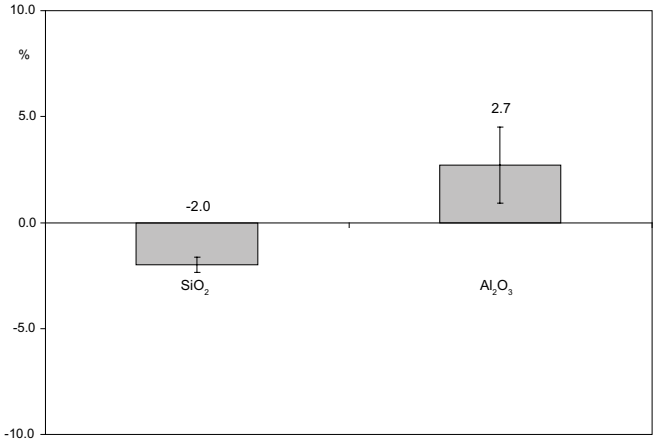

Figure 5-16. *Mean relative changes in SiO_2 ,and Al_2O_3 content in altered rock compared to fresh rock, values normalized to measured mass change. Error bars are 1σ standard deviations for the altered samples.*

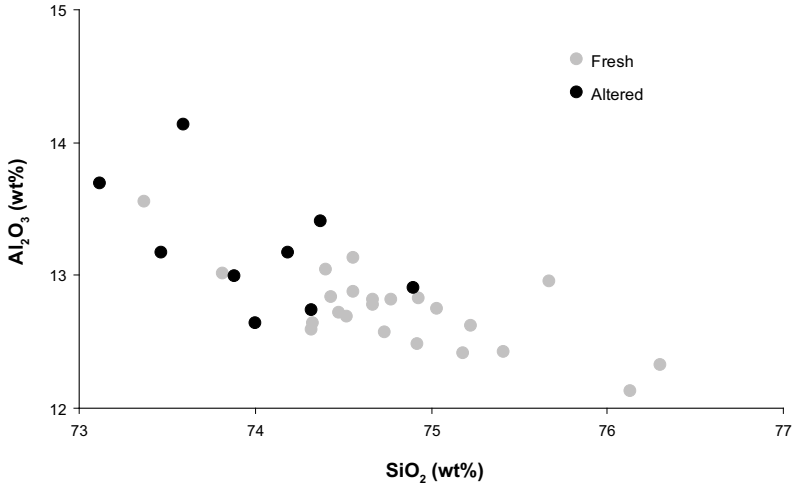

Figure 5-17. *SiO_2 versus Al_2O_3 for fresh and altered rock.*

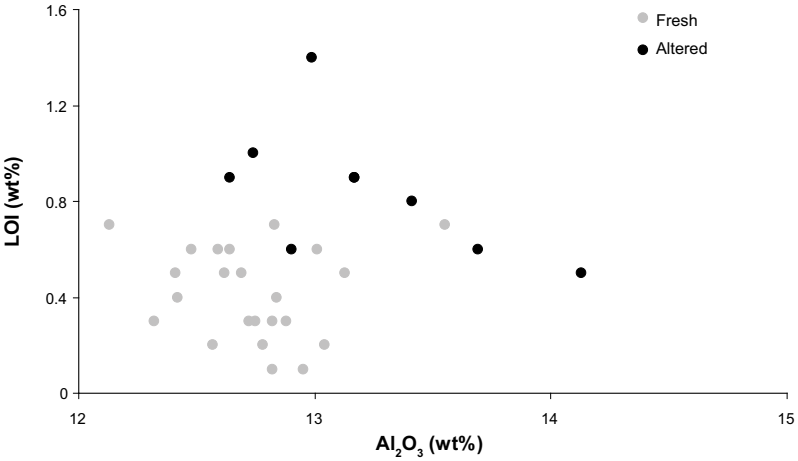

Figure 5-18. *Al_2O_3 versus LOI for fresh and altered rock.*

K, Rb, Ba, Cs

These elements are mainly hosted in K-feldspar, micas and clay minerals. The K_2O increases in the altered rock which can be seen as crystallization of adularia and sericite in the saussuritized plagioclase. Rb shows a positive correlation with K in both fresh and altered rock. The high standard deviation for Rb, makes the mean positive relative change in Figure 5-19 non-representative. However, in Figure 5-20 a decrease in Rb content compared to the fresh rock, is more evident than an increase. Normally Ba has a positive correlation with K, however in Forsmark the altered samples with the highest K_2O content show low Ba content (Figure 5-21). This could be explained by that the newly crystallized adularia and sericite contains low concentrations of Ba, since lower formation temperature normally gives less room for substitution, due to a more rigid lattice structure. The decrease in Cs is not significant, as seen in Figure 5-22, but since Cs preferably is hosted in biotite, the chloritization process of the biotite may very well lead to a decrease in Cs in the altered rock.

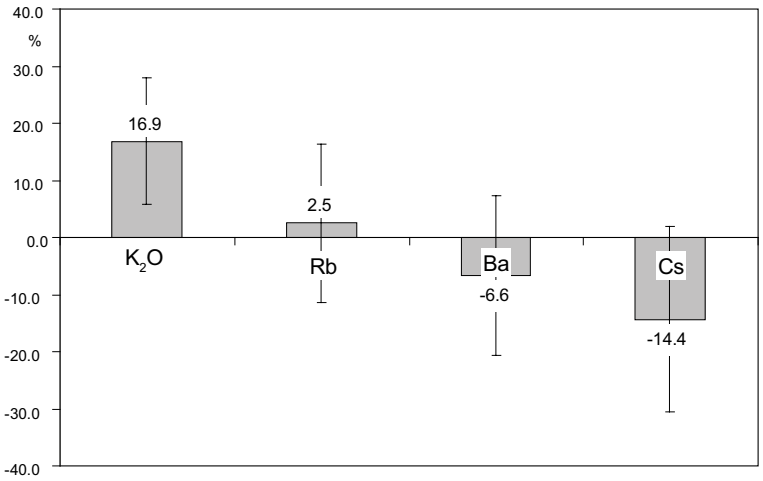

Figure 5-19. *Mean relative changes in K_2O, Rb, Ba and Cs content in altered rock compared to fresh rock, values normalized to measured mass change. Error bars are 1σ standard deviations for the altered samples for the altered samples.*

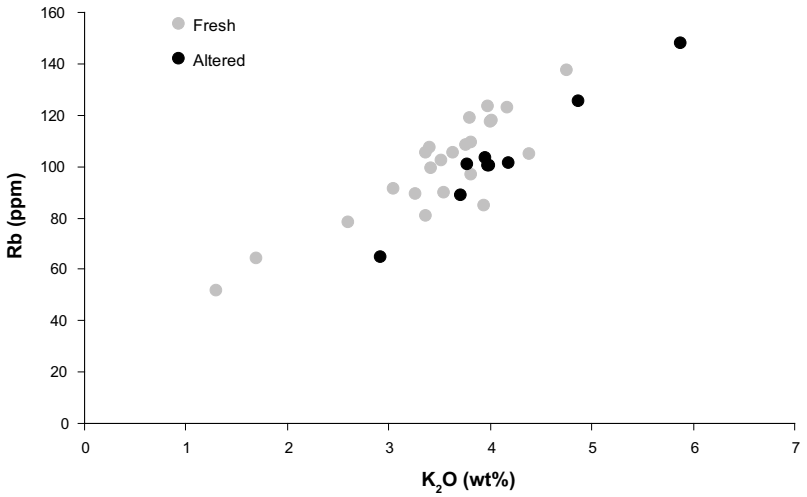

Figure 5-20. *K_2O versus Rb for fresh and altered rock.*

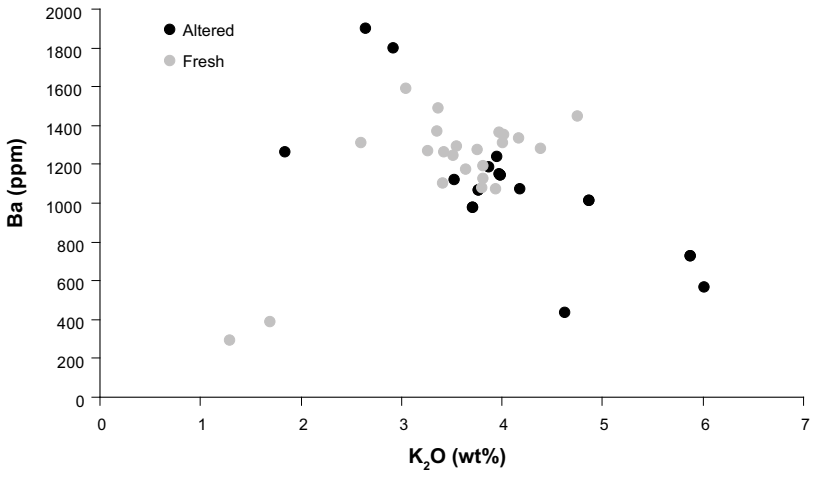

Figure 5-21. *K_2O versus Ba in fresh and altered whole rock samples.*

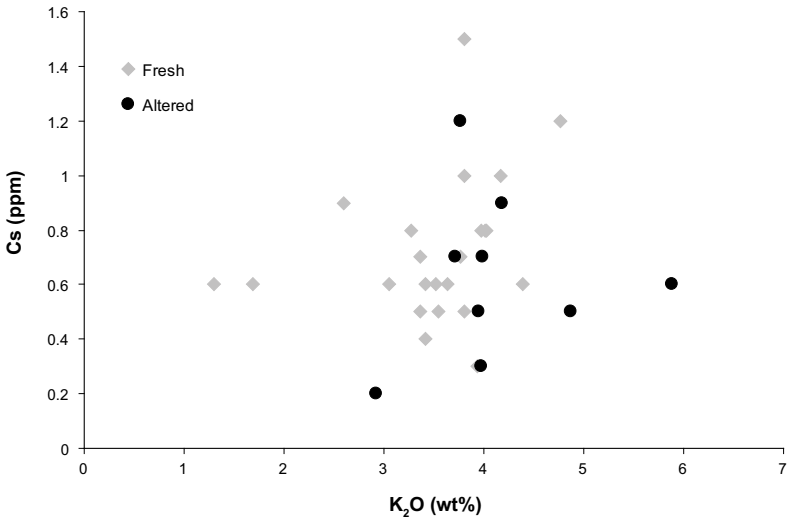

Figure 5-22. *K_2O versus Cs in fresh and altered whole rock samples.*

Ca, Na, Sr

The mean CaO content decreases, although the standard deviation is large, as seen in Figure 5-23 and 5-24. The CaO decrease is associated with the breakdown of the anorthosite component of oligoclase. And since Sr substitute for Ca in oligoclase, the decrease in Sr is also associated with this process. The three samples in Figure 5-25 with the highest Sr/CaO ratio (marked with arrows) are the samples with the highest epidote content, according to the modal analyses of thin sections. The geochemical analyse of an epidote-sealed fracture network has the highest Sr content of all samples (see Section 5-5), indicating epidote as one of the most Sr rich minerals. Na_2O increases in the altered rock due to the albite replacement of oligoclase.

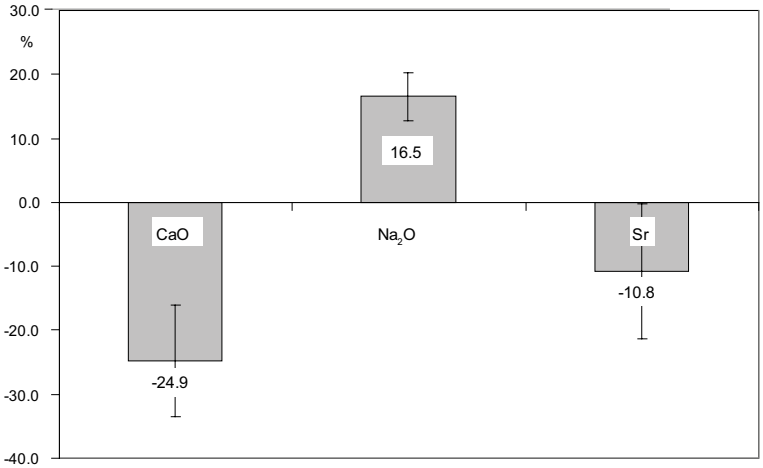

Figure 5-23. *Mean relative changes in CaO, Na_2O and Sr content in altered rock compared to fresh rock, values normalized to measured mass change. Error bars are 1σ standard deviations for the altered samples.*

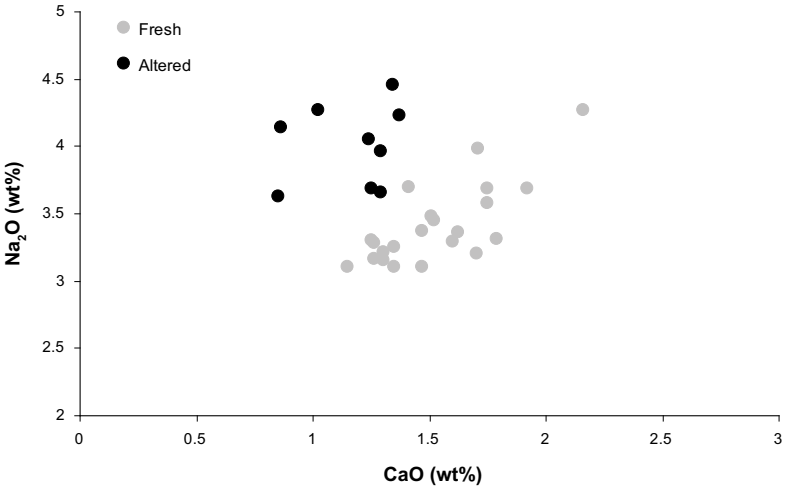

Figure 5-24. *CaO versus Na_2O content in fresh and altered rock.*

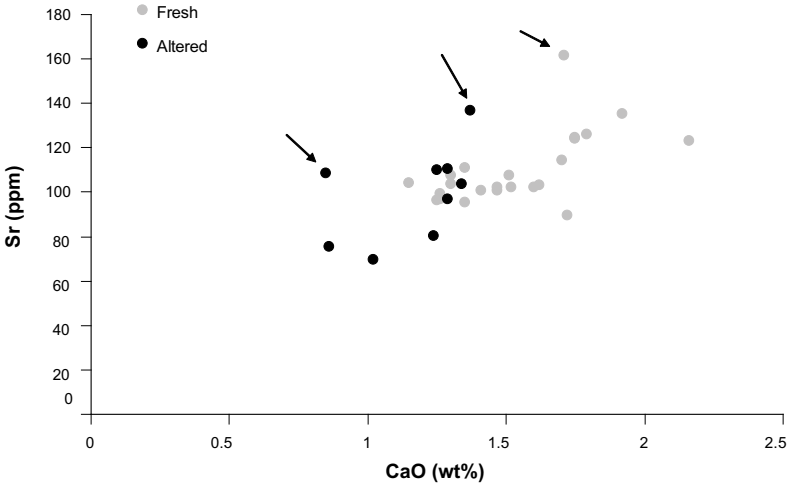

Figure 5-25. *CaO versus Sr content in fresh and altered rock. The samples marked with arrows have the highest epidote content based on point counting of all analysed samples.*

Fe, Mg, Mn, Ti, V, Sc

Both the mean total Fe (given as Fe_2O_3) and MgO content have decreased in the altered rock compared to the fresh rock samples (Figure 5-26), although it is only the Fe depletion that is evident when the variation of the fresh and altered populations is considered (Figure 5-27). The main Mg and Fe minerals in the fresh and altered rock are biotite and chlorite. Both Fe_2O_3 and MgO were made mobile during the chloritization of biotite but most of the Fe_2O_3 and MgO were incorporated in the chlorite that replaced the biotite although the Mg/Fe ratio is lower in the chlorite than in the biotite (Figure 5-8). The decrease in Fe in the altered rock is surprising since the chlorite contains more Fe than the biotite which is the main Fe-carrying mineral in the rock. The decrease could be the result of breakdown of magnetite.

A rough calculation based on the biotite content of KFM02A 949.87 m from the point counting together with SEM-EDS analyses of the biotite in this sample gives a calculated Fe_2O_3 of ~ 1.84 wt% (the density of biotite varies between 2.7 and 3.3 g cm^{-3} /Deer et al. 1992/ which is close to the density of the granitic rock so the volume% from the point counting has been assumed to represent an approximate weight%). When the other two main Fe-bearing minerals are added, which are epidote which contains ~ 12 wt% Fe_2O_3 and magnetite which contain ~ 70 wt% Fe (all opaque minerals have been assumed to be magnetite), the Fe_{total} given as

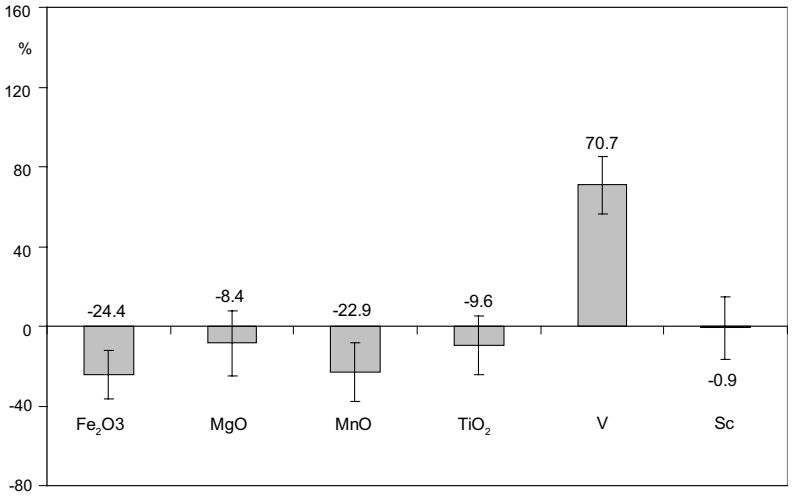

Figure 5-26. *Mean relative changes in Fe_2O_3, MgO, Mn, Ti, V and Sc content in altered rock compared to fresh rock, values normalized to measured mass change. The mean values are not representative for all elements (see text). Error bars are 1σ standard deviations for the altered samples.*

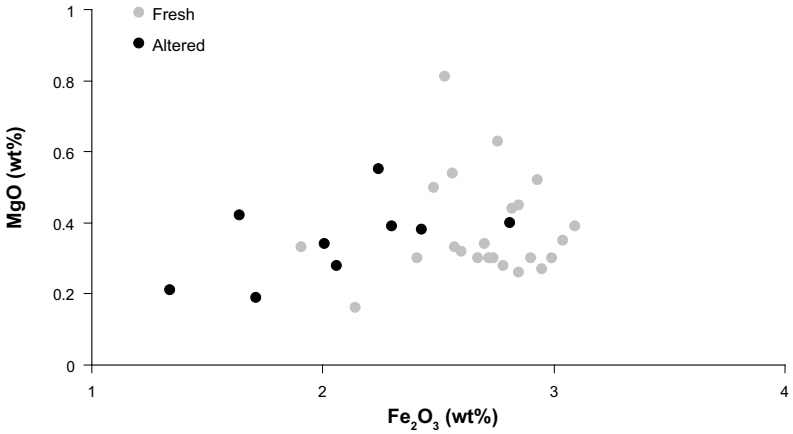

Figure 5-27. *Fe_2O_3 versus MgO content in fresh and altered rock.*

Fe_2O_3 is still only ~ 2.0 wt% which is lower than the measured Fe_2O_3 content in the whole rock (2.95 wt%). When the same calculation is made for sample KFM01A 521.27 m, which has a slightly higher biotite and epidote content, concordance between the whole rock Fe_2O_3 content of 2.53 wt% and the calculated value of 2.49 wt% is better. This supports that biotite, epidote and magnetite are the main Fe-carrying minerals in the rock. The rather bad correspondence in some samples may be a result of how the thin section is cut in relation to the rock foliation, which should influence the biotite content more than the content other minerals during point counting. Inhomogeneous epidote distribution may also influence the results as well as minor phases of e.g. titanite and allanite.

Ti is often seen as an immobile element, at least on the macro scale. No change in Ti content can be seen between the fresh and altered samples from Forsmark, only one altered sample has a TiO_2 content lower than the fresh rock sample with the lowest TiO_2 content (Figure 5-28). On the micro-scale, however Ti mobility can be seen by the formation of titanite lenses in the chloritized biotite.

No clear change in the MnO content can be seen in the altered rock although a few samples show slightly lower MnO contents giving a lower mean value (Figure 5-26 and 5-29). The increase in V is of low significance since the concentrations are so low (Figure 5-30) and no change can be shown for Sc (Figure 5-31).

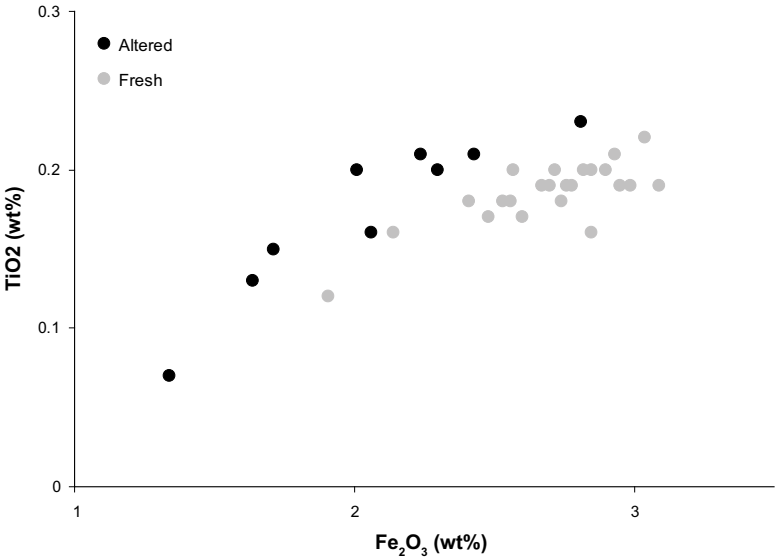

Figure 5-28. *Fe_2O_3 versus TiO_2 content in fresh and altered rock.*

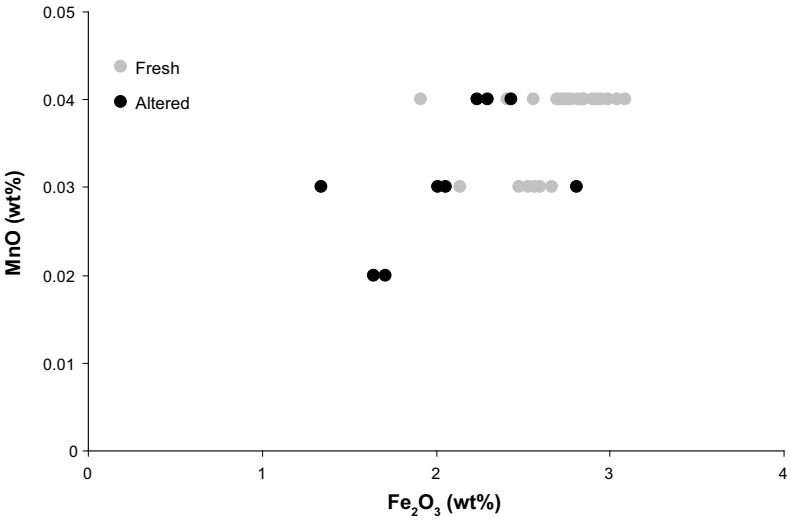

Figure 5-29. *Fe_2O_3 versus MnO content in fresh and altered rock.*

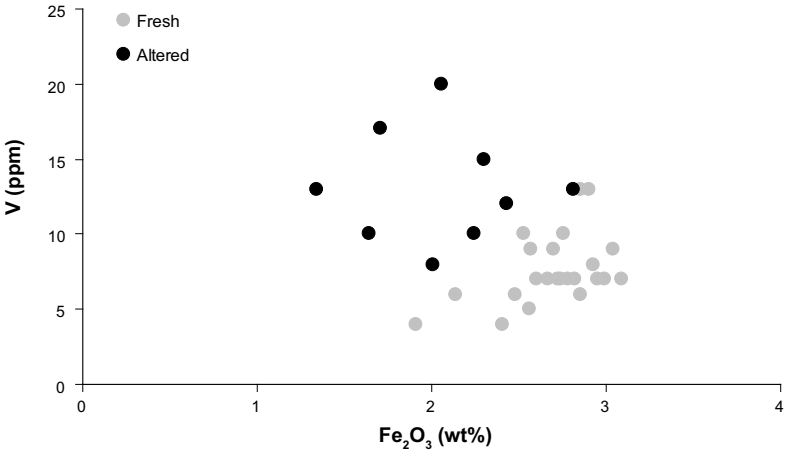

Figure 5-30. *Fe_2O_3 versus V content in fresh and altered rock.*

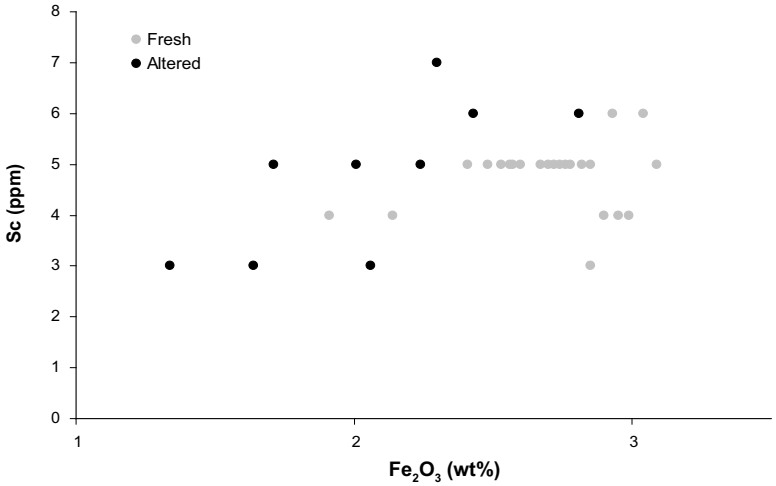

Figure 5-31. *Fe_2O_3 versus Sc content in fresh and altered rock.*

P

No real change in P_2O_5 content can be seen between altered and fresh samples although the normalized mean value (Table 5-2) but the low concentrations makes the mean value unreliable.

S, Zn, Cu, As, Sb

Analyses of sulphur of both fresh and altered rock are presented in Table 5-1.

Sulphur, Zn, Cu, As and Sb are normally associated with sulphides. In the analysed samples no correlation can be seen between these elements, except for in KFM02A 949.90–950.10 m which has a S content of 2,790 ppm and also show a high Cu content (Figure 5-32). This indicates the presence of a Cu-sulphide although no mineralogical evidence for this can be seen in the thin section. No correlation can be seen between S content and alteration of the rock and the

Table 5-1. Sulphur content in fresh and altered rock.

Sample	Sample type	Rock code	S (ppm)
KFM01B 52.01	Epidote network	–	<8
KFM01B 434.33	Laumontite network	–	124
KFM01B 397.41	Fresh	101057	31.7
KFM07A 183.13A	Fresh	101057	79.8
KFM08B 91.36A	Fresh	101057	59
KFM01B 41.89	Altered	101057	<8
KFM01B 416.50	Altered	101057	81.8
KFM02A 495.64	Altered	101057	9.31
KFM02A 502.64	Altered	101051	<8
KFM02A 503.78	Altered	101051	8.96
KFM07A 183.13R	Altered	101057	63.8
KFM08A 623.13R	Altered	101057	10.8
KFM08B 91.36R	Altered	101057	37.8
KFM01B 36.66	Altered	101057	<8
KFM01A 521.10	Fresh	101051	229
KFM02A 712.05	Fresh	101057	20.7
KFM02A 949.90	Fresh	101057	2,790
KFM09A 150.67	Fresh	101051	30.4
KFM09A 172.45	Fresh	101051	26.4

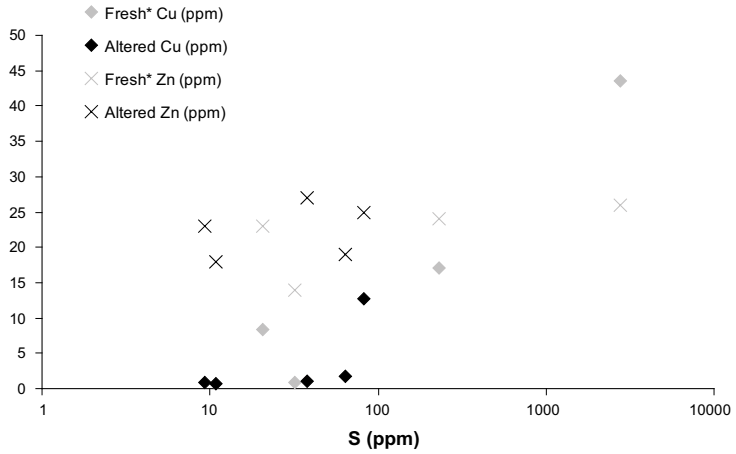

Figure 5-32. *S content versus Cu and Zn in fresh and altered rock.*

variation in S content is probably due to inhomogeneity in the rock. The non-correlation of sulphur with the alteration is in agreement with the absence of coeval sulphide fracture minerals indicating low mobility of sulphur during the hydrothermal alteration event.

U, Th

The main U and Th hosting minerals in the rock-type are zircon, titanite and allanite. Both U and Th show enrichment in the altered rock (Figure 5-33) but the standard deviations are very large and no conclusions can be drawn from the data as shown in Figure 5-34. Since the samples with high U content are from both fresh and altered samples, this variation is probably due to heterogeneity in distribution of the U and Th bearing minerals. The U/Th ratios in all samples are relatively similar except in one altered sample which indicates enrichment in Th. Two samples, one fresh and one altered, show higher U content than the other samples (Figure 5-34).

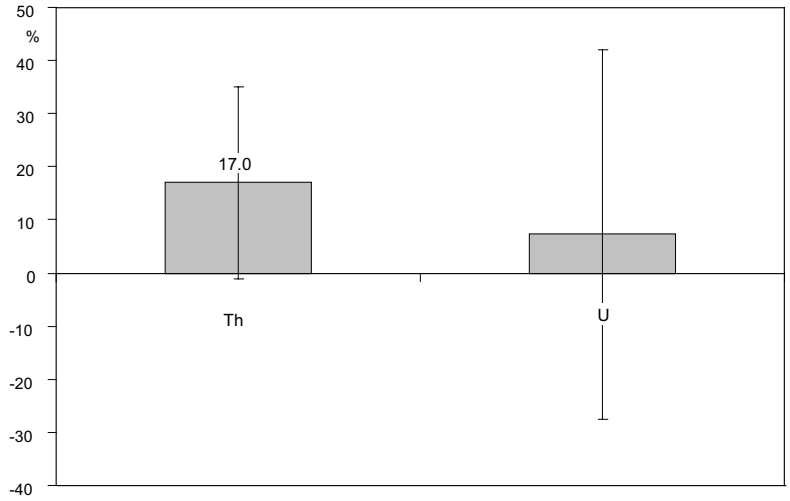

Figure 5-33. *Mean relative change in Th and U concentration in altered rock compared to fresh rock, the values have been normalized based on measured mass change. The Error bars are 1σ standard deviations for the altered samples.*

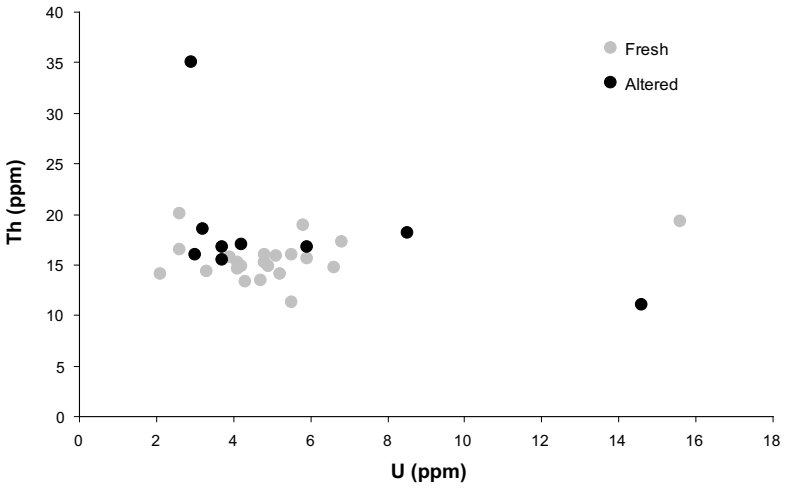

Figure 5-34. *U versus Th content in fresh and altered rock.*

REE, Y

In granitic rocks REEs are mainly concentrated in accessory minerals like titanite, apatite and allanite. Theses minerals tend to concentrate the light REEs resulting in typical granitic LREEs enrichment signatures /Clark 1984, Grauch 1989/. No considerable change in REE content can be seen between the fresh and altered rock (Figure 5-35 and 5-36), although a small decrease in Eu can be seen due to the alteration and break down of plagioclase. A small increase in Ce is also evident, probably associated with a somewhat more favourable precipitation of Ce^{4+} in the oxidizing environment prevailing during the hydrothermal alteration event.

Y behaves similar as the HREEs, due to similarity in ionic size as shown in Figure 5-37.

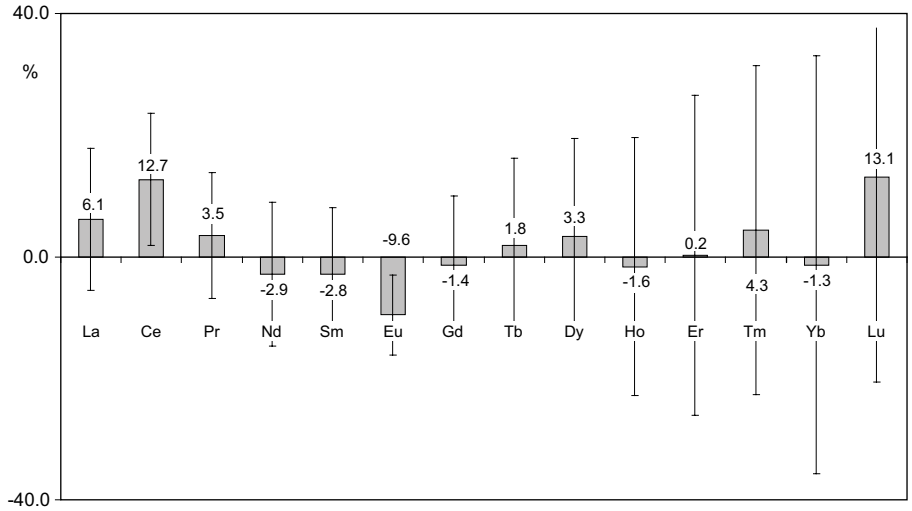

Figure 5-35. *Mean relative change in REEs between fresh and altered rock, the values have been normalized based on the measured mass change. Error bars are 1σ standard deviations for the altered samples.*

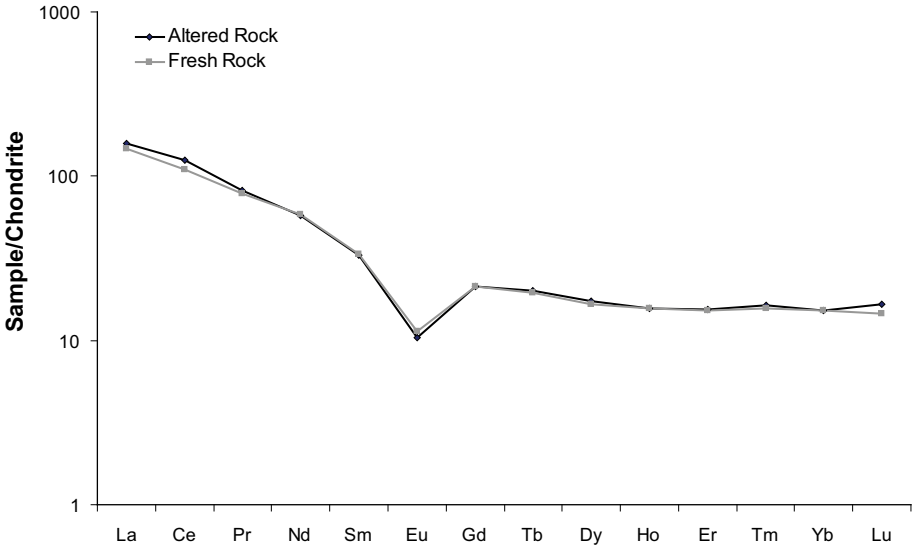

Figure 5-36. *Chondrite normalized REE diagram of mean whole rock values for fresh and altered rock. Fresh rock values from /Petersson et al. 2004, 2005/, chondrite values from /Evansen et al. 1978/.*

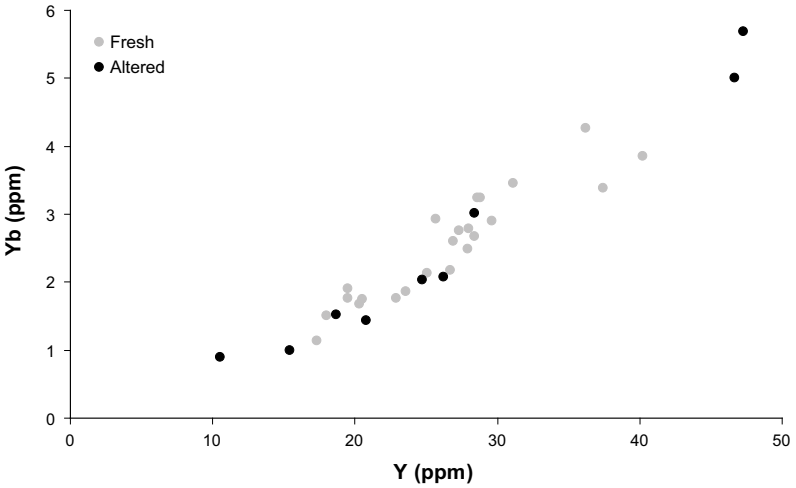

Figure 5-37. *Y versus Yb content in fresh and altered rock.*

Table 5-2. Mean whole rock chemistry of fresh and altered medium-grained metagranite to metagranodiorite (rock code 101057). Mean fresh rock values have been calculated based on data from /Petersson et al. 2004, 2005/. Std = Standard deviation, n.a. = not analysed, n(fresh) = 23, n(altered) = 9.

	Fresh	Std	Altered	Std		Fresh	Std	Altered	Std		Fresh	Std	Altered	Std		Fresh	Std	Altered	Std
SiO_2 (wt%)	**74.80**	0.66	**73.77**	0.87	Ag (ppm)	**<0.10**	n.a.	**0.10**	0.00	Rb	**100.25**	19.88	**97.89**	27.25	La (ppm)	**36.14**	2.86	**34.40**	6.64
Al_2O_3	**12.74**	0.30	**13.41**	0.44	As	**<0.50**	n.a.	**<0.5**	n.a.	Sb	**0.10**	0.02	**0.10**	0.00	Ce	**70.48**	5.70	**72.76**	14.38
Fe_2O_3	**2.70**	0.28	**2.15**	0.52	Ba	**1,199.60**	300.44	**1,132.06**	316.30	Sc	**4.78**	0.67	**4.89**	1.54	Pr	**7.53**	0.64	**7.25**	1.35
MgO	**0.38**	0.14	**0.34**	0.11	Be	**n.a.**	n.a.	**1.89**	0.33	Se	**<0.5**	n.a.	**<0.5**	n.a.	Nd	**27.76**	2.21	**25.16**	4.81
CaO	**1.54**	0.25	**1.37**	0.41	Bi	**<0.1**	n.a.	**<0.1**	n.a.	Sn	**<0.1**	n.a.	**1.78**	0.44	Sm	**5.19**	0.41	**4.71**	0.95
Na_2O	**3.41**	0.29	**3.88**	0.22	Cd	**2.01**	1.26	**<0.1**	n.a.	Sr	**110.07**	16.19	**114.29**	27.22	Eu	**0.66**	0.04	**0.58**	0.08
K_2O	**3.51**	0.78	**4.05**	0.90	Co	**2.62**	0.57	**2.26**	0.55	Ta	**0.60**	0.21	**0.68**	0.19	Gd	**4.38**	0.43	**4.18**	0.95
TiO_2	**0.19**	0.02	**0.17**	0.05	Cs	**0.72**	0.27	**0.71**	0.23	Tl	**0.18**	0.09	**0.13**	0.06	Tb	**0.73**	0.08	**0.73**	0.21
P_2O_5	**0.03**	0.01	**0.05**	0.01	Cu	**22.28**	23.50	**2.03**	4.04	Th	**15.52**	1.98	**18.08**	6.81	Dy	**4.23**	0.70	**4.23**	1.30
MnO	**0.04**	0.00	**0.03**	0.01	Ga	**15.18**	0.62	**15.03**	1.26	U	**5.10**	2.58	**5.71**	3.80	Ho	**0.89**	0.19	**0.86**	0.31
Cr_2O_3	**n.a.**	n.a.	**0.01**	0.00	Hf	**4.48**	0.48	**4.60**	0.77	V	**7.61**	2.33	**12.89**	3.69	Er	**2.54**	0.61	**2.42**	1.15
LOI	**0.42**	0.19	**0.80**	0.28	Hg	**1.97**	2.53	**<0.01**	n.a.	W	**0.44**	0.29	**1.07**	0.63	Tm	**0.40**	0.12	**0.39**	0.19
TOT/C	**0.03**	0.02	**0.05**	0.03	Mo	**1.53**	2.51	**0.42**	0.41	Zr	**152.35**	16.91	**141.44**	31.26	Yb	**2.53**	0.81	**2.28**	1.31
TOT/S	**0.06**	0.11	**0.01**	0.01	Nb	**11.19**	1.08	**9.19**	1.48	Y	**26.50**	6.04	**24.97**	10.74	Lu	**0.37**	0.12	**0.38**	0.22
SUM	**99.74**	0.11	**100.04**	0.14	Ni	**2.73**	1.82	**1.10**	0.27	Zn	**26.17**	3.96	**24.56**	9.36					
S (ppm)	**n.a.**	n.a.	**57.48**	33.73	Pb	**2.64**	2.11	**3.91**	2.63	Au (ppb)	**2.18**	2.97	**2.54**	0.51					

Fine- to medium-grained metagranitoid (rock code 101051)

The wide span of different rock types within the group with rock code 101051, makes a comparison between the altered and fresh rock geochemistry difficult. The only two altered samples selected from this rock group are of granitic composition and represent end-members of this rock group. The mean geochemistry of fresh and altered rock is presented in Table 5-3 but the large difference between the fresh and altered rock is due to differences in rock type and not to alteration. The trends seen in Figure 5-38 and 5-39 represent a gradual transition from granitic to tonalitic composition of the parent rock with e.g. more SiO_2 and less Fe_2O_3 and MgO in the more granitic parent rock of the altered samples. The inhomogeneity of the rock group can also be seen in the REE diagram (Figure 5-40). Due to the inhomogeneity of the reference rock, no real comparison can be made between the fresh and altered rock, hence only the raw data of the altered rock is presented in this report (Table 5-3).

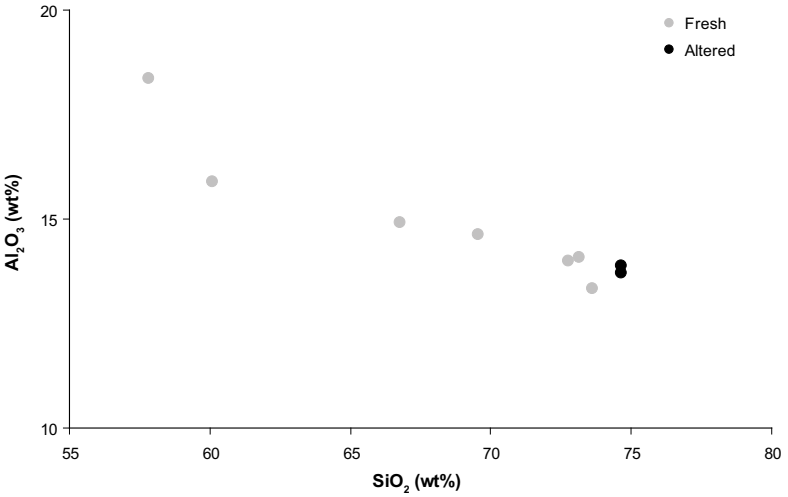

Figure 5-38. *SiO_2 versus Al_2O_3 content in fresh and altered rock.*

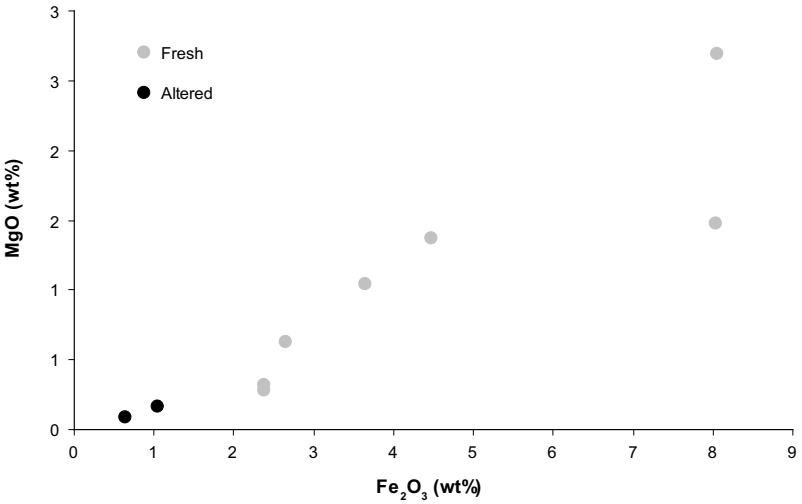

Figure 5-39. *Fe_2O_3 versus MgO content in fresh and altered rock.*

Table 5-3. Mean whole rock chemistry of fresh and altered fine- to medium-grained metagranitoid (rock code 101051). Mean fresh rock values have been calculated based on data from /Petersson et al. 2004, 2005/. Std = Standard deviation, n.a. = not analysed, n(fresh) = 8, n(altered) = 2. The altered samples are both granitic while the fresh rock is a mean value of the whole span of the rock group, hence the large difference between fresh and altered rock.

	Fresh	Std	Altered	Std		Fresh	Std	Altered	Std		Fresh	Std	Altered	Std		Fresh	Std	Altered	Std
SiO_2 (wt%)	**67.69**	6.45	**74.66**	0.01	Ag (ppm)	**<0.10**	n.a.	**<0.10**	n.a.	Rb	**81.44**	41.14	**129.65**	17.61	La (ppm)	**38.83**	14.58	**16.80**	3.82
Al_2O_3	**15.03**	1.68	**13.80**	0.11	As	**0.50**	0.00	**<0.5**	n.a	Sb	**0.10**	0.00	**<0.1**	n.a.	Ce	**74.50**	29.52	**32.65**	7.28
Fe_2O_3	**4.52**	2.52	**0.84**	0.28	Ba	**746.17**	195.75	**500.85**	91.71	Sc	**10.29**	8.86	**2.00**	0.00	Pr	**7.86**	2.96	**3.30**	0.73
MgO	**1.12**	0.84	**0.13**	0.05	Be	**n.a.**	n.a.	**1.50**	0.71	Se	**<0.5**	n.a.	**<0.5**	n.a.	Nd	**29.03**	10.37	**10.85**	2.05
CaO	**3.98**	2.24	**1.03**	0.33	Bi	**0.11**	0.04	**<0.1**	n.a.	Sn	**<0.1**	n.a.	**<1.0**	n.a.	Sm	**5.17**	2.15	**2.10**	0.42
Na_2O	**3.70**	0.48	**3.78**	0.16	Cd	**2.83**	0.41	**<0.1**	n.a.	Sr	**377.11**	276.55	**111.40**	11.60	Eu	**1.01**	0.32	**0.46**	0.01
K_2O	**2.48**	1.46	**5.32**	0.98	Co	**7.81**	6.31	**<0.5**	n.a.	Ta	**0.74**	0.34	**0.45**	0.21	Gd	**4.11**	1.97	**1.94**	0.18
TiO_2	**0.42**	0.26	**0.05**	0.02	Cs	**0.80**	0.16	**0.70**	0.28	Tl	**0.24**	0.13	**<0.1**	n.a.	Tb	**0.61**	0.32	**0.35**	0.01
P_2O_5	**0.12**	0.09	**0.02**	0.00	Cu	**13.91**	8.96	**0.55**	0.07	Th	**14.70**	11.28	**9.10**	1.41	Dy	**3.32**	1.69	**2.01**	0.27
MnO	**0.07**	0.05	**0.02**	0.01	Ga	**18.69**	2.64	**17.95**	0.05	U	**4.04**	2.44	**14.95**	4.74	Ho	**0.66**	0.34	**0.44**	0.08
Cr_2O_3	**n.a.**	n.a.	**0.01**	0.00	Hf	**4.53**	1.48	**2.75**	0.21	V	**41.71**	47.13	**<6**	n.a.	Er	**1.83**	0.94	**1.34**	0.27
LOI	**0.59**	0.23	**0.65**	0.21	Hg	**1.54**	3.28	**<0.01**	n.a.	W	**0.34**	0.19	**0.35**	0.07	Tm	**0.30**	0.14	**0.25**	0.06
TOT/C	**0.03**	0.02	**0.14**	0.16	Mo	**0.46**	0.21	**0.40**	0.00	Zr	**157.57**	48.23	**60.15**	5.30	Yb	**1.95**	0.89	**1.52**	0.49
TOT/S	**0.04**	0.03	**0.01**	0.00	Nb	**10.72**	5.35	**8.30**	1.13	Y	**20.19**	10.01	**13.50**	1.70	Lu	**0.31**	0.15	**0.23**	0.01
SUM	**99.72**	0.07	**100.29**	0.04	Ni	**3.56**	2.39	**0.70**	0.14	Zn	**52.00**	16.57	**18.00**	8.49					
S (ppm)	**n.a.**	n.a.	**<8.96**	n.a.	Pb	**3.47**	3.86	**6.40**	0.14	Au (ppb)	**0.84**	0.50	**2.10**	0.28					

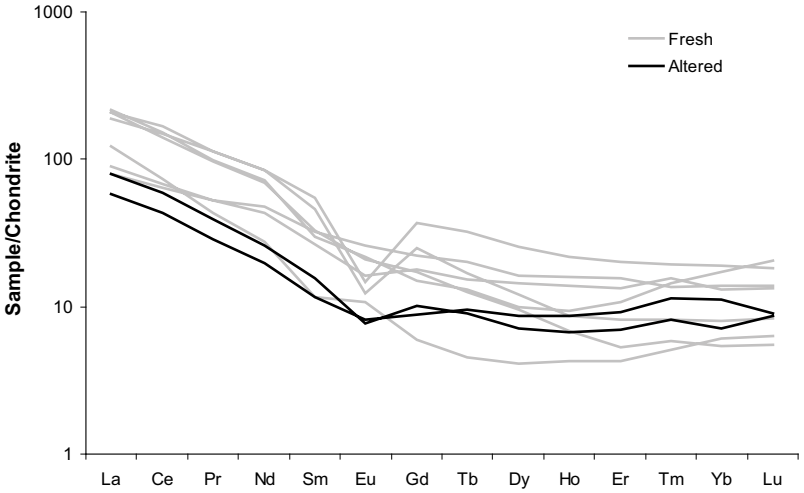

Figure 5-40. *Chondrite normalized REE diagram of whole rock samples for fresh and altered rock. Fresh rock values from /Petersson et al. 2004, 2005/, chondrite values from /Evansen et al. 1978/.*

5.3 Porosity and density

Porosity in crystalline rock is dominated by voids created by micro-fractures but also intra-granular pores in secondary minerals, fluid inclusions, and porosity between grains /e.g. Tullborg and Larson 2006 and references therein/. The connected porosity measured with the water saturation techniques and density results are presented in Table 5-4.

Table 5-4. Connected porosity and density of fresh and altered rock.

Drill core	Depth	Sample type	Intensity of alteration	Rock code	Porosity (%)	Dry density (g/cm3)
KFM01A	103.31	Fresh		101057	0.49	2.6634
KFM01A	312.92	Fresh		101057	0.45	2.6504
KFM01A	350.50	Fresh		101057	0.50	2.6538
KFM01A	704.00	Fresh		101057	0.49	2.6567
KFM01B	397.41	Fresh		101057	0.56	2.6447
KFM02A	953.68	Fresh		101057	0.55	2.6508
KFM04A	694.65	Fresh		101057	0.56	2.6502
KFM09A	150.67	Fresh		101051	0.44	2.6407
KFM09A	172.45	Fresh		101051	0.48	2.6398
KFM01B	36.66	Altered	Faint	101057	0.75	2.6343
KFM01B	37.41	Altered	Faint	101057	0.77	2.6305
KFM01B	416.50	Altered	Medium	101057	0.93	2.6196
KFM02A	483.64	Altered	Not ox. in Boremap	101057	0.50	2.6381
KFM02A	495.64	Altered	Faint	101057	0.64	2.6187
KFM02A	500.35	Altered	Weak	101051	0.62	2.6126
KFM02A	503.78	Altered	Faint	101051	0.59	2.6172
KFM02A	506.80	Altered	Faint	101057	0.44	2.6362

Medium-grained metagranite to metagranodiorite (rock code 101057)

The porosity of the unaltered medium-grained metagranite to metagranodiorite (rock code 101057) varies between 0.45 and 0.56% with a mean of 0.51% ± 0.04 (1σ), the porosity of the same, but altered rock type varies between 0.44 and 0.93% with a mean of 0.67% ± 0.18 (1σ) (Figure 5-42). The large variation in porosity in the altered rock (Figure 5-43) is among other things due to the different intensity of the alteration. Two of the altered samples, KFM02A 483.64 m and KFM02A 506.80 m, show no increase in porosity at all compared to the fresh rock. The sample with the highest porosity has also been mapped in Boremap as the most intensely altered sample (Table 5-4). The dry density decreases from a mean of 2.653g cm^{-3} ± 0.006 (1σ) for the fresh rock to a mean of 2.630g cm^{-3} ± 0.008 (1σ) for the altered rock.

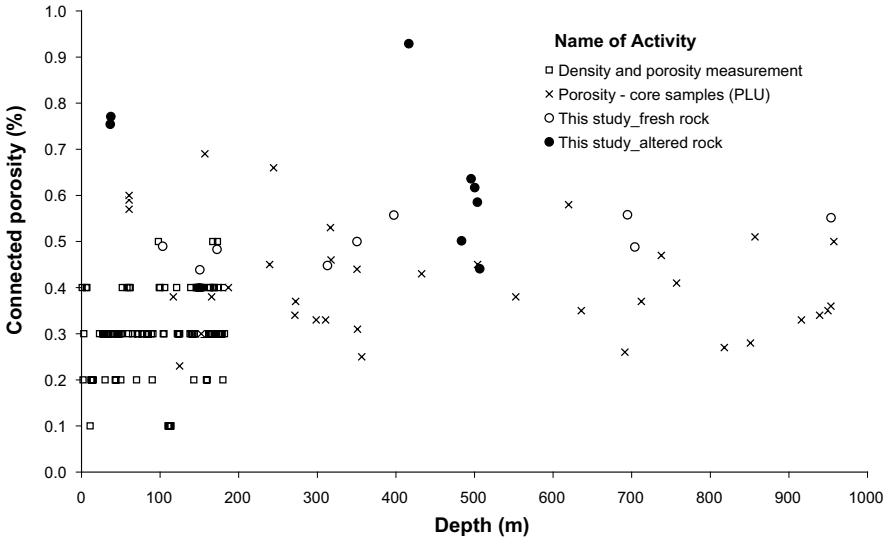

Figure 5-41. *Comparison of porosities versus depth for a selection of different activities including porosity measurements carried out within the site investigation program (including this study), data from SKB data base SICADA. The porosity of all samples in the plot has been measured by the water saturation technique at the SP laboratory although different sample sizes have been used in some of the activities. The results have also been reported with different degrees of precision.*

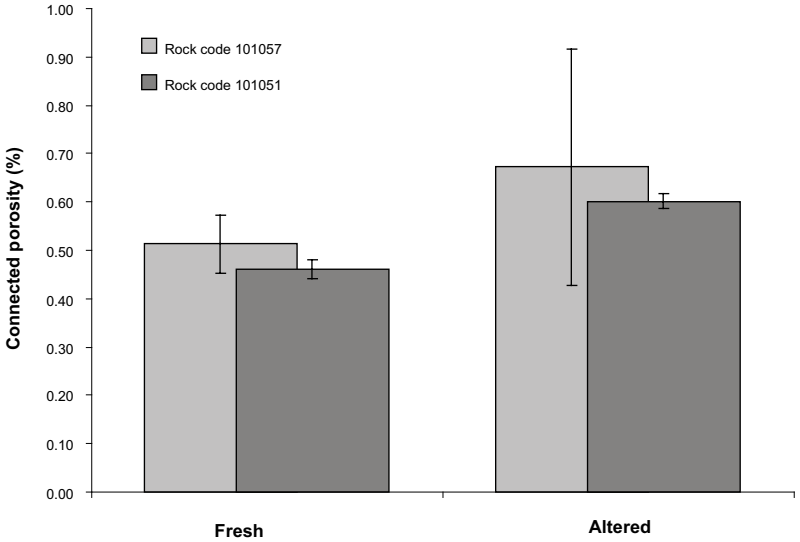

Figure 5-42. *Mean porosity of medium-grained metagranite to metagranodiorite (rock code 101057) and fine- to medium-grained metagranitoid (rock code 101051) of fresh and altered rock. Error bars are the total variation in porosity.*

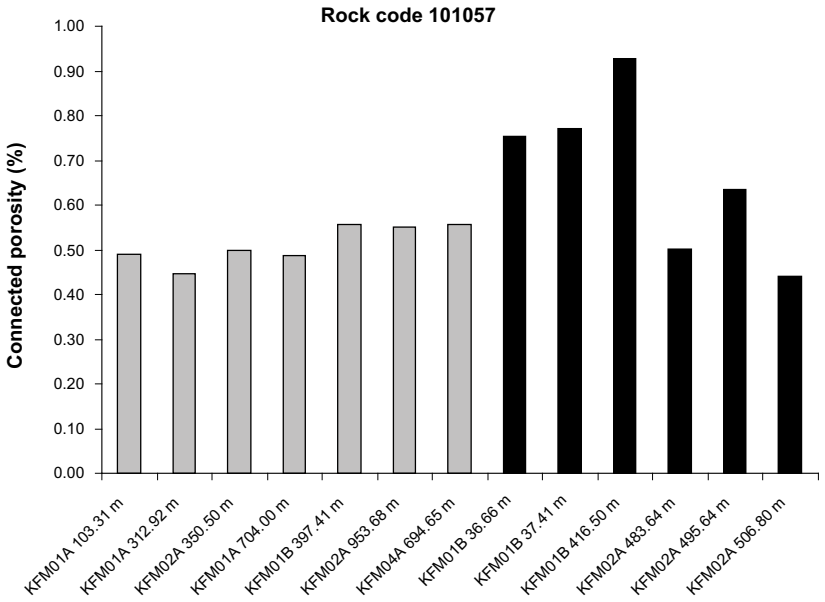

Figure 5-43. *Porosity for the analysed samples of fresh and altered medium-grained metagranite to metagranodiorite (rock code 101057).*

Fine- to medium-grained metagranitoid (rock code 101051)

The porosities of the analysed fine- to medium-grained metagranitoid (rock code 101051) are 0.44 and 0.48% with a mean of 0.46% ± 0.03 (1σ) for the two fresh samples and 0.59 and 0.62% with a mean of 0.60% ± 0.02 (1σ) for the two altered samples. The dry density of the analysed fresh rock samples are 2.641 and 2.640g cm^{-3} and for the altered rock samples 2.613 and 2.617g cm^{-3}.

Since the porosity has been measured as the connected porosity, the cause of the higher porosity in the altered rock is mainly due to an increase in micro fractures but also the increased intra-granular porosity in the chloritized biotite. Since chlorite often occurs as clusters, and the rock is foliated, the chlorite grains are often connected and provide migration pathways for fluids through the rock sample (Figure 5-44). The increased intra-granular porosity in the altered plagioclase (see Section 5.1), probably has a minor influence on the measured porosity since these pores only are connected to a low degree as seen in Figure 5-4. The decrease in density is associated with increased porosity.

Figure 5-44. *Scanned thin section with connected chlorite grains. The base of the figure is ~ 1.5 cm, KFM02A 506.80 m.*

5.4 Redox capacity

The redox capacity of fresh and altered rock gained from the Mössbauer analyses is presented in Table 5-5 as the oxidation factor for silicates ($Fe^{3+}_{silicate} / (Fe^{2+} + Fe^{3+})_{silicate}$) and as the total oxidation factor (($Fe^{3+}_{silicate} + Fe^{3+}_{oxide}$) / Fe_{total}). The oxide content in the rock is too small to allow a presentation of the oxidation factor for the oxides separately, but they are included in the total oxidation factor.

Medium-grained metagranite to metagranodiorite (rock code 101057)

One sample (KFM02A 949.20 m) of fresh rock has been contaminated with metallic iron and is therefore excluded from the calculation of mean values.

The Mössbauer analyses show that most Fe^{3+} is found in chlorite and biotite. Due to the overlap in the Mössbauer spectrum between many hydrated Fe-Mg mineral spectra, it is difficult to separate chlorite from biotite, but from the microscopical studies it is evident that biotite dominate in the fresh samples, while chlorite has completely replaced biotite in the altered samples (Section 5.1). Epidote is also present in various amounts in all analysed samples and since epidote only contains Fe^{3+} it has a large impact on the oxidation factor of the rock. The oxidation factor of the silicates in the fresh rock varies between 0.11 and 0.25 with a mean of 0.16 ± 0.07 (1σ), and in the altered rock between 0.08 and 0.24 with a mean of 0.17 ± 0.06 (1σ). The mean oxidation factor is larger in the altered rock but the difference is very small.

The Fe-oxides identified are magnetite, hematite and possibly goethite. The oxide content is small in the rock and is often only seen as trace amounts in the Mössbauer analyses. Since hematite has an oxidation factor of 1 and magnetite 0.67, the presence of these oxides has a large influence on the total oxidation factor.

The total oxidation factor varies between 0.18 and 0.38 in the fresh rock with a mean of 0.24 ± 0.09 (1σ). In the altered rock, the oxidation factor varies between 0.15 and 0.36 with a mean of 0.28 ± 0.07 (1σ) (Figure 5-45). If the fresh sample with the highest oxidation factor is excluded (KFM07A 183.13A which in thin section show alteration, marked with arrow in Figure 5-45) the mean oxidation factor for the fresh samples is 0.20 ± 0.02 (1σ). This mean value is considered more reliable than the former.

The increase in mean total oxidation factor from 0.20 to 0.28, shows that the altered rock is more oxidized than the fresh rock, although the change is very small. The value of 0.28 for the altered rock shows that the Fe^{2+} content still is higher than the Fe^{3+} content in the altered rock.

A small increase in the oxidation degree can be seen in the altered rock although the change is so small that the term *oxidized wall rock* is somewhat misleading for the altered rock since most of the iron still is in the Fe^{2+} oxidation state.

Fine- to medium-grained metagranitoid (rock code 101051)

The oxidation factor varies highly between the samples. The variation is mainly due to variation in mineralogy; e.g. KFM02A 502.64 m which has a high silicate oxidation factor of 0.42 contains only 0.8 volume % chlorite (and no biotite) and since chlorite contains more Fe^{2+} than Fe^{3+}, this increases the oxidation factor. A mean value for this rock type would be deceptive due to the large variation and the results are presented in Table 5-5. The oxidation factors do not seem to differ significantly from the values of the medium-grained metagranite to metagranodiorite (rock code 101057).

Table 5-5. Mössbauer spectroscopy results. Chl = chlorite and/or biotite, ep = epidote, mt = magnetite, hm = hematite, goeth = goethite, tr = trace amounts, Met Fe = metallic Fe. Where no total oxidation factor is available due to low oxide content, the silicate oxidation factor has been used for Fe^{2+} calculations.

Borehole	Depth (m)	Sample type	Rock code	Fe^{3+} Mineral	Oxidation factor (silicate)	Oxidation factor (total)	Fe_{total} (wt%)	Fe^{2+} (wt%)
KFM02A	712.05	Fresh	101057	chl, ep, tr, mt, hm	0.18	0.22	1.73	1.35
KFM02A	949.90	Fresh	101057	chl, ep, Met Fe	0.21		1.79	
KFM07A	183.13O	Fresh	101057	chl, tr, oxides	0.11	0.18	2.09	1.71
KFM08A	623.13O	Fresh	101057	chl, ep, mt, hm	0.25	0.38	1.78	1.11
KFM08B	91.36O	Fresh	101057	chl, ep, tr, mt	0.11	0.19	1.76	1.42
KFM01A	521.10	Fresh	101051	chl, ep, goeth, tr, oxides	0.33	0.40	1.85	1.11
KFM09A	150.67	Fresh	101051	chl, ep, tr, oxides	0.23		n.a.	
KFM09A	172.45	Fresh	101051	chl, ep, tr, mt	0.18	0.24	n.a.	
KFM01B	36.66	Altered	101057	chl, hm, tr, mt	0.08	0.15	1.44	1.22
KFM01B	416.50	Altered	101057	chl, ep, mt	0.12	0.26	1.61	1.19
KFM02A	483.64	Altered	101057	chl, ep	0.19		1.15	0.93
KFM02A	495.64	Altered	101057	chl, ep, mt, hm	0.23	0.31	0.94	0.65
KFM02A	506.80	Altered	101057	chl, ep, mt, hm	0.21	0.34	1.57	1.03
KFM07A	183.13R	Altered	101057	chl, ep, tr, oxides	0.16	0.24	1.41	1.07
KFM08A	623.13R	Altered	101057	chl, ep, mt	0.24	0.36	1.97	1.26
KFM08B	91.36R	Altered	101057	chl, ep, tr, mt	0.17	0.29	1.70	1.21
KFM02A	502.64	Altered	101051	chl, ep, tr, oxides	0.43		0.45	0.26
KFM02A	503.78	Altered	101051	chl, ep, tr, oxides	0.16	0.23	0.73	0.56

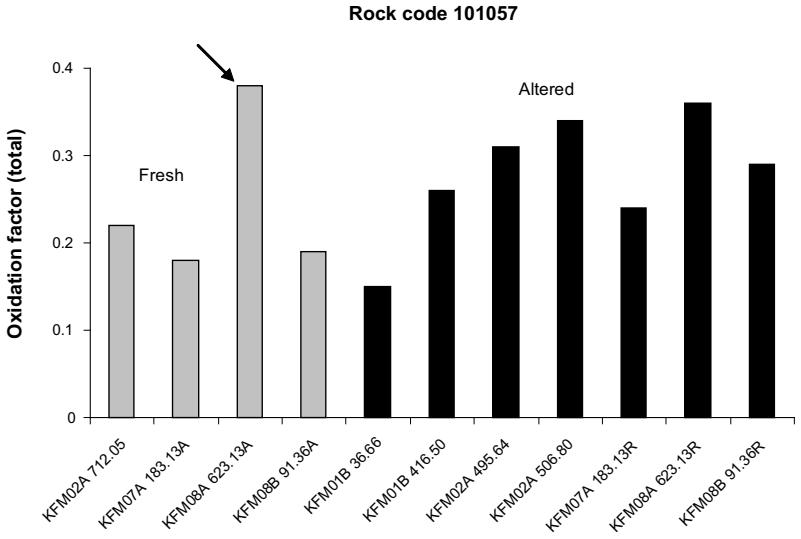

Figure 5-45. *Total oxidation factor ($(Fe^{3+}_{silicate} + Fe^{3+}_{oxide})/ Fe_{total}$) of fresh and altered samples from medium-grained metagranite to metagranodiorite (rock code 101057) where a total oxidation factor is available, the sample with an arrow have been excluded from the calculation of mean values due to evidence of alteration (see text).*

5.5 Epidote and laumontite sealed fracture networks

One sample each of an epidote and laumontite sealed fracture network has been analysed for geochemistry and redox capacity. Both are common in the Forsmark area, especially in deformation zones (Figure 5-46 and 5-47).

Whole rock geochemistry of the sealed networks is presented in Appendix 2. SiO_2, Fe_2O_3 and MgO decreases slightly compared to the mean values of the fresh rock while CaO, K_2O and Al_2O_3 increases. The most evident change in trace element geochemistry is an increase in Sr from ~ 110 ppm in the fresh rock to 335.1 ppm in the epidote sealed network. Of the trace elements the largest decrease is in the Cs, Cu, Ni and Mo content while Ga and V increases. However, the concentrations of trace elements are overall low and the changes are therefore not significant. The REEs are relatively unchanged (Figure 5-48). Epidote contains dominantly Fe^{3+} /Deer et al 1992/ which also can be seen by the high silicate oxidation factor in the analysed sample (Table 5-6).

The most evident change in the analyses of laumontite sealed fracture network is the increase in LOI to 2.2 wt% compared to the medium-grained metagranite to metagranodiorite (rock code 101057) host rock. SiO_2 and Fe_2O_3 decreases slightly compared to the mean values of the fresh rock while CaO, K_2O and Al_2O_3 increases. Of the trace elements the largest decrease is in the Cu, Ni and Mo content while V, W and Sc increases. However, the concentrations of trace elements are overall low and the changes are therefore unreliable. The REEs are relatively unchanged (Figure 5-48). The oxidation factor of the laumontite sealed fracture network is slightly higher than the fresh rock (Table 5-6), mostly due to the presence of small sub-microscopic grains of hematite in the laumontite. Nevertheless, the oxidation factor reveals that most iron still is in the Fe^{2+} oxidation state.

Figure 5-46. *Epidote sealed fracture network. The diameter of the drill core is c 5 cm. KFM01B 52.01–52.34 m.*

Figure 5-47. *Laumontite sealed fracture network. The diameter of the drill core is c 5 cm. KFM01B 434.33–434.70 m.*

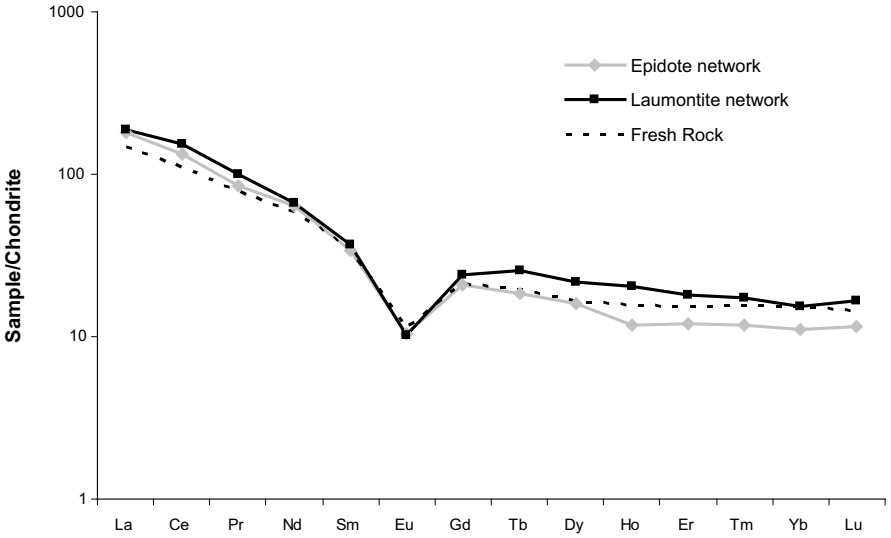

Figure 5-48*. Chondrite normalized REE diagram of fracture networks sealed with epidote and laumonite. Mean fresh rock values (medium-grained metagranite to metagranodiorite, rock code 101057) from /Petersson et al. 2004, 2005/, chondrite values from /Evansen et al. 1978/.*

Table 5-6. Mössbauer spectroscopy results of epidote and laumontite sealed fracture networks. Chl = chlorite and/or biotite, ep = epidote, hm = hematite. Where no total oxidation factor is availible due to low oxide content, the silicate oxidation factor has been used for Fe^{2+} calculations.

Borehole	Depth (m)	Sample type	Rock code	Fe3+ Mineral	Oxidation factor (silicate)	Oxidation factor (total)	Fe_{tot} (wt%)	Fe2+ (wt%)
KFM01B	52.01	Epidote network	–	ep, chl	0.78		1.69	0.37
KFM01B	434.33	Laumontite network	–	chl, ep, hm.	0.27	0.42	1.01	0.59

6 Summary and discussion

The major mineralogical changes in the altered rock are the almost complete saussuritization of plagioclase and chloritization of biotite. The red colour in the altered rock is due to sub-microscopic grains of hematite within the saussuritized plagioclase and along the grain boundaries. A small increase in the epidote content can be seen in the altered rock while the K-feldspar is relatively unaffected.

Most elements have been relatively immobile during the hydrothermal alteration, although redistribution of many elements on the micro-scale has occurred which can be seen mineralogically. The main trends are an increase in K, Na and LOI (Lost on Ignition) while Ca and Fe decrease in the altered rock. The rock generally contains very low concentrations of trace elements and the mobility has been small for most trace elements. A small decrease in Sr can be seen which is associated with the decrease in Ca due to the breakdown of plagioclase. No mobility of U and Th has been shown except for one sample which has been enriched in Th. The REE content does not differ significantly between the fresh and altered rock.

The connected porosity increases in the altered rock and is mainly due to micro-fractures and an increase in inter-granular porosity due to chloritization of biotite. The saussuritized plagioclase has an increased intra-granular porosity, although this is probably not seen in the porosity data, since most of these pores are not connected.

The redox capacity of the altered rock is slightly lower than in the fresh rock although the difference is small. The mean total oxidation factor increases from 0.20 in the fresh rock to 0.28 in the altered rock showing that most iron still is in the Fe^{2+} oxidation state in the altered rock.

The altered red-stained rock is exclusively associated with the two oldest generations of fracture fillings at the Forsmark site; Generation 1 which consists of mainly epidote, quartz and chlorite and the hydrothermal sequence of fracture minerals named Generation 2 which is dominated by adularia, prehnite, laumontite, calcite and chlorite /Sandström and Tullborg 2006/.

Generation 1 is interpreted to be older than 1,704–1,635 Ma based on epidote stability and $^{40}Ar/^{39}Ar$ cooling ages of biotite /Page et al. 2004, Sandström and Tullborg 2006/. $^{40}Ar/^{39}Ar$ dating of fracture filling adularia from Generation 2 gives ages between ~ 1,100 and 1,000 Ma /Sandström et al. 2006/. These ages can also be assigned to the rock alteration since the alteration is closely associated with the fractures with minerals from these Generations. E.g. is chlorite with the same Fe/Mg ratio found in both fractures and altered wall rock, prehnite and laumontite which are found as fracture minerals are also found in the altered wall rock as lenses in chloritized biotite.

7 Acknowledgement

We would like to thank the Assen Simeonov (SKB) and Michael Stephens (SGU) at Forsmark for support and Jesper Petersson (Vattenfall Power Consultant AB) and Kenneth Åkerström (KÅ Geoskog) for assistance during the drill core sampling. Allan Stråhle (Geosigma AB) and the staff at SICADA are thanked for assistance with the SICADA data. Hans Annersten (Uppsala University) is thanked for the Mössbauer analyses and Ulf Brising (Sweco Position) for GIS support. Sven Åke Larson (Göteborg University) is thanked for reviewing the report and Henrik Drake (Göteborg University) for discussions regarding the alteration in the Oskarshamn area.

References

Baker J H, 1985. Rare earth and other trace element mobility accompanying albitization in a Proterozoic granite, W. Bergslagen, Sweden. Mineralogical Magazine, 49, 107–115.

Clark A M, 1984. Mineralogy of the Rare Earth Elements, *In* P. Henderson (ed.): Rare Earth Element Geochemistry, Elsevier Scientific, 33–61.

Deer W A, Howie R A, Zussman J, 1992. An introduction to the rock-forming minerals. 2nd ed. Longman Scientific & Technical. 696 pp.

Drake H, Tullborg E-L, 2006b. Oskarshamn site investigation. Mineralogical, chemical and redox features of red-staining adjacent to fractures – Results from drill cores KSH01A+B and KSH03A+B. SKB P-06-01, Svensk Kärnbränslehantering AB.

Drake H, Sandström B, Tullborg E L, 2006. Mineralogy and geochemistry of rocks and fracture fillings from Forsmark and Oskarshamn: Compilation of data for SR-Can. R-report in progress, Svensk Kärnbränslehantering AB.

Drake H, Tullborg E-L, 2006a. Oskarshamn site investigation. Mineralogical,chemical and redox features of red-staining adjacent to fractures – Results from drill core KLX04. SKB P-06-02, Svensk Kärnbränslehantering AB.

Eliasson T, 1993. Mineralogy, geochemistry and petrophysics of red coloured granite adjacent to fractures. SKB TR 93-06. Svensk Kärnbränslehantering AB.

Evansen N M, Hamilton P J, O'Nions R K, 1978. Rare Earth Abundances in Chondritic Meteorites. Geochimica et Cosmochimica Acta, 42, 1199–1212.

Grant J A, 1986. The Isocon diagram – a simple solution to Gresen's equation for metasomatic alteration. Economic Geology, 81, 1976–1982.

Grauch R I, 1989. Rare Earth Elements in metamorphic rocks, *In* B.R. Lipin and G.A. McKay (eds.): Reviews in Mineralogy, vol 21, Geochemistry and Mineralogy of Rare Earth Elements, 147–167.

Gresen R L, 1967. Composition-volume relationship of metasomatism. Chemical Geology, 2, 47–65.

Parneix J C, Beaufort D, Dudoignon P, Meunier A, 1985. Biotite chloritization process in hydrothermally altered granites. Chemical Geology, 51, 89–101.

Page L, Hermansson T, Söderlund P, Andersson J, Stephens M B, 2004. Forsmark site investigation. Bedrock mapping U-Pb, $^{40}Ar/^{39}Ar$ and (U-Th)/He geochronology. SKB P-04-126. Svensk Kärnbränslehantering AB.

Petersson J, Tullborg E-L, Mattsson H, Thunehed H, Isaksson H, Berglund J, Lindroos H, Danielsson P, Wängnerud A, 2004. Forsmark site investigation. Petrography, geochemistry, petrophysics and fracture mineralogy of boreholes KFM01A, KFM02A and KFM03A+B. SKB P-04-103, Svensk Kärnbränslehantering AB.

Petersson J, Berglund J, Wängerud A, Stråhle A, 2005. Forsmark site investigation. Petrographic and geochemical characteristics of bedrock samples from boreholes KFM04A-06A, and a whitened alteration rock. SKB P-05-156, Svensk Kärnbränslehantering AB.

Sandström B, Savolainen M, Tullborg E-L, 2004. Forsmark site investigation. Fracture Mineralogy. Results from fracture minerals and wall rock alteration in boreholes KFM01A, KFM02A, KFM03A and KFM03B. SKB P-04-149, Svensk Kärnbränslehantering AB.

Sandström B, Tullborg E-L, 2005. Forsmark site investigation. Fracture mineralogy. Results from fracture minerals and wall rock alteration in KFM01B, KFM04A, KFM05A and KFM06A. SKB P-05-197, Svensk Kärnbränslehantering AB.

Sandström B, Tullborg E-L, 2006. Forsmark site investigation. Fracture mineralogy. Results from fracture minerals in KFM06B, KFM06C, KFM07A, KFM08A and KFM08B. SKB P-06-226, Svensk Kärnbränslehantering AB.

Sandström B, Page L, Tullborg E-L, 2006. Forsmark site investigation. Geochronology of fracture minerals. SKB P-06-213, Svensk Kärnbränslehantering AB.

SKB, 2005. Preliminary site description. Forsmark area – version 1.2. SKB R-05-18, Svensk Kärnbränslehantering AB.

SKB, 2006. Site descriptive modelling. Forsmark stage 2.1. Feedback for completing of the site investigation including input from safety assessment and repository engineering. SKB R-06-38, Svensk Kärnbränslehantering AB.

Stephens M B, Lundqvist S, Ekström M, Bergman T, Anderson J, 2003. Forsmark site investigation. Bedrock mapping: Rock types, their petrographic and geochemical characteristics, and a structural analysis of the bedrock based on stage 1 (2002) surface data. SKB P-03-75, Svensk Kärnbränslehantering AB.

Tullborg E-L, Larson S Å, 2006. Porosity in crystalline rocks – A matter of scale. Engineering Geology, 84, 75–83.

Appendix 1

Sample descriptions

KFM01A 312.92 m

Sample type: Fresh rock
Rock code: 101057

KFM01A 704.00 m

Sample type: Fresh rock
Rock code: 101057

KFM01B 36.66–37.15 m

Sample type: Altered rock
Rock code: 101057
Degree of oxidation in Boremap: Faint

KFM01B 37.41–37.80 m

Sample type: Altered rock
Rock code: 101057
Degree of oxidation in Boremap: Faint

KFM01B 41.89–42.05 m

Sample type: Altered Rock
Rock code: 101057
Degree of oxidation in Boremap: Medium

KFM01B 52.01–52.34 m

Sample type: Epidote network
Rock code: 101057

KFM01B 397.41–397.76 m

Sample type: Fresh rock
Rock code: 101057

KFM01B 416.50–416.77 m

Sample type: Altered rock
Rock code: 101057
Degree of oxidation in Boremap: Medium

KFM01B 434.33–434.70 m

Sample type: Laumontite network
Rock code: 101057

KFM02A 350.50–350.60 m

Sample type: Fresh rock
Rock code: 101057

KFM02A 483.64–483.97 m

Sample type: Altered rock
Rock code: 101057
Degree of oxidation in Boremap: Not oxidized in Boremap

KFM02A 495.64–495.88 m

Sample type: Altered rock
Rock code: 101057
Degree of oxidation in Boremap: Faint

KFM02A 500.35–500.55 m

Sample type: Altered rock
Rock code: 101051
Degree of oxidation in Boremap: Week

KFM02A 502.64–502.85 m

Sample type: Altered rock
Rock code: 101051
Degree of oxidation in Boremap: Faint

KFM02A 503.78–503.97 m

Sample type: Altered rock
Rock code: 101051
Degree of oxidation in Boremap: Faint

KFM02A 506.80–507.10 m

Sample type: Altered rock
Rock code: 101057
Degree of oxidation in Boremap: Faint

KFM02A 953.68–953.78 m

Sample type: Fresh rock
Rock code: 101057

KFM04A 694.65–694.80 m

Sample type: Fresh rock
Rock code: 101057

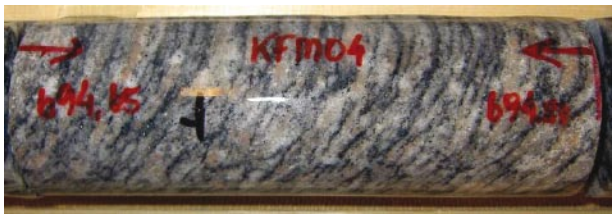

KFM07A 183.13–183.41 m

Sample type: Fresh and Altered rock
Rock code: 101057
Degree of oxidation in Boremap: Faint

KFM08A 623.03–623.35 m

Sample type: Fresh and altered rock
Rock code: 101057
Degree of oxidation in Boremap: Faint

KFM08B 91.36–91.58 m

Sample type: Altered rock
Rock code: 101057
Degree of oxidation in Boremap: Not oxidized in Boremap

Appendix 2

Whole rock geochemistry

Sample	KFM01B 52.01	KFM01B 434.33	KFM01B 397.41	KFM01B 397.41Re	KFM02A 915.8	KFM03A 311.33	KFM07A 183.13A	KFM08A 623.13A
Sample type	**Epidote Network**	**Laumontite Network**	**Fresh**	**Fresh**	**Fresh**	**Fresh**	**Fresh**	**Fresh**
Rock code			101057	101057	101051	101051	101057	101057
SiO_2 wt%	72.02	72.73	74.48	75.09	59.86	57.8	71.85	74.02
Al_2O_3	13.29	13.08	13.11	13.11	15.82	17.12	13.93	13
Fe_2O_3	2.41	1.44	1.8	1.66	7.87	9.14	2.99	2.55
MgO	0.13	0.39	0.24	0.21	2.84	1.79	0.34	0.31
CaO	3.37	2.18	1.7	1.64	7.3	6.44	1.8	2.11
Na_2O	3.44	3.48	3.61	3.56	3.48	3.37	3.83	4.04
K_2O	4.22	4.27	4.17	3.97	1.21	1.92	3.87	2.65
TiO_2	0.2	0.15	0.14	0.13	0.49	0.98	0.22	0.21
P_2O_5	0.05	0.03	0.03	0.03	0.16	0.3	0.05	0.05
MnO	0.03	0.03	0.03	0.03	0.15	0.14	0.04	0.02
Cr_2O_3	0.014	0.003	0.009	0.009	0.016	0.011	0.013	0.012
LOI	0.9	2.2	0.6	0.6	0.6	1	1	0.8
TOT/C	0.22	0.06	0.06	0.06	0.01	0.01	0.02	0.01
TOT/S	0.01	0.01	0.01	0.01	0.01	0.01	0.05	0.01
SUM	100.08	99.98	99.92	100.05	99.81	100.02	99.94	99.77
S ppm	<8	124	31.7	n.a.	n.a.	n.a.	79.8	n.a.
Ag	<.1	<.1	<.1	<.1	<.1	<.1	<.1	<.1
As	<.5	<.5	<.5	0.5	<.5	<.5	<.5	<.5
Ba	1,119.7	1,133.4	1,637.6	1,600.4	867.2	713.4	1,182.1	1,896.4
Be	2	2	2	2	2	1	2	2
Bi	<.1	0.1	<.1	<.1	0.2	<.1	<.1	<.1
Cd	<.1	0.1	<.1	<.1	<.1	<.1	<.1	<.1
Co	1.9	1.9	1.7	2	17.5	15.7	2.6	2.4
Cs	0.3	0.6	0.4	0.3	0.8	1.2	0.8	0.5
Cu	0.9	2.9	0.8	1	2.9	5.6	0.9	0.5
Ga	21.1	12.2	15.6	14.9	16.8	19.9	14.1	15.3
Hf	5.5	4.9	3.9	3.5	2.8	2.8	4.6	4.8
Hg	<.01	<.01	<.01	<.01	<.01	<.01	<.01	<.01
Mo	0.3	0.1	0.8	1	0.3	0.2	0.5	0.3
Nb	8	7	8.8	8.9	6.2	10.4	10	8.9
Ni	0.8	1	0.8	0.9	1.9	1.1	1.1	1.2
Pb	1.6	2.9	3.7	3.5	1.7	2.2	3.2	2.6
Rb	111.3	90.7	82.9	81.6	36.9	62.9	85.5	53.6
Sb	<.1	<.1	<.1	<.1	<.1	<.1	<.1	<.1
Sc	5	12	5	4	24	27	6	6
Se	<.5	<.5	<.5	<.5	<.5	<.5	<.5	<.5
Sn	2	1	2	1	2	1	2	2
Sr	335.1	92	140.7	140.8	321.5	341.4	117.8	172.2
Ta	0.4	0.3	1	0.6	0.4	0.6	0.7	1
Tl	<.1	<.1	0.1	0.1	0.1	0.3	0.1	0.1
Th	13.3	20	13.5	12	8.2	6.5	18.2	14.1
U	6.7	4.3	13.5	13	2.7	2	5.7	3.2
V	22	15	14	16	150	33	10	11
W	0.8	1	0.2	0.5	0.9	0.8	0.5	0.3
Zr	192.7	158.6	117.4	97.4	90.7	99.6	148.1	160.2
Y	20.8	30.2	29.5	28	22.2	29.5	31.2	31.2
Zn	10	18	14	14	30	68	23	14
Au ppb	1	1.7	2.9	2	1.4	1.2	1.7	2.7

Sample	KFM01B 52.01	KFM01B 434.33	KFM01B 397.41	KFM01B 397.41Re	KFM02A 915.8	KFM03A 311.33	KFM07A 183.13A	KFM08A 623.13A
Sample type	**Epidote Network**	**Laumontite Network**	**Fresh**	**Fresh**	**Fresh**	**Fresh**	**Fresh**	**Fresh**
La ppm	44.2	46.1	25.5	24	24.1	25.8	37.2	36.5
Ce	84	98.3	53.1	46	52.6	56	84.8	74.6
Pr	8.21	9.65	5.43	4.7	5.69	6.82	8.63	7.56
Nd	30.2	31.8	19.5	17.2	21.1	25.1	31.8	27.4
Sm	5.2	5.7	3.7	3.7	4.2	5	5.7	5
Eu	0.61	0.59	0.53	0.6	0.87	1.46	0.68	0.54
Gd	4.27	4.91	3.58	3.4	3.81	5.06	5.05	4.28
Tb	0.69	0.96	0.68	0.63	0.67	0.87	0.96	0.76
Dy	4.08	5.51	4.54	4.26	3.54	5.51	5.43	4.89
Ho	0.67	1.15	0.94	0.95	0.78	1.08	1.09	1.01
Er	1.98	2.98	2.79	2.73	2.05	2.8	3.22	2.93
Tm	0.3	0.44	0.5	0.48	0.34	0.44	0.52	0.5
Yb	1.84	2.54	3.44	3.14	2.39	2.52	2.91	3.46
Lu	0.29	0.42	0.58	0.51	0.39	0.45	0.5	0.5

Sample	KFM08B 91.36A	KFM01B 36.66	KFM01B 41.89	KFM01B 416.5	KFM02A 483.64	KFM02A 495.64	KFM02A 502.64	KFM02A 503.78
Sample type	**Fresh**	**Altered**	**Altered**	**Altered**	**Altered**	**Altered**	**Altered**	**Altered**
Rock code	101057	101057	101057	101057	101057	101057	101051	101051
SiO_2 wt%	74.03	73.88	73.12	74.9	74.37	73.59	74.67	74.65
Al_2O_3	13.43	12.99	13.69	12.9	13.41	14.13	13.88	13.72
Fe_2O_3	2.51	2.06	1.71	2.3	1.64	1.34	0.64	1.04
MgO	0.34	0.28	0.19	0.39	0.42	0.21	0.09	0.16
CaO	1.54	1.25	1.37	0.86	1.29	0.85	0.79	1.26
Na_2O	3.78	3.69	4.23	4.14	3.96	3.63	3.66	3.89
K_2O	3.53	4.18	4.87	3.71	3.99	5.88	6.01	4.63
TiO_2	0.21	0.16	0.15	0.2	0.13	0.07	0.03	0.06
P_2O5	0.06	0.04	0.04	0.05	0.04	0.03	0.02	0.02
MnO	0.04	0.03	0.02	0.04	0.02	0.03	0.01	0.02
Cr_2O_3	0.013	0.005	0.007	0.017	0.013	0.014	0.012	0.011
LOI	0.6	1.4	0.6	0.6	0.8	0.5	0.5	0.8
TOT/C	0.1	0.06	0.08	0.07	0.02	0.03	0.03	0.25
TOT/S	0.01	0.01	0.01	0.01	0.01	0.01	0.01	0.01
SUM	100.08	99.96	99.99	100.11	100.09	100.28	100.31	100.26
S ppm	59	<8	<8	81.8	n.a.	9.31	<8	8.96
Ag	<.1	0.1	<.1	<.1	<.1	<.1	<.1	<.1
As	<.5	<.5	<.5	<.5	<.5	<.5	<.5	<.5
Ba	1,118.2	1, 069.9	1,012.9	976.4	1,142.8	723.8	565.7	436
Be	2	2	2	2	2	1	1	2
Bi	<.1	<.1	<.1	<.1	<.1	<.1	<.1	<.1
Cd	<.1	<.1	<.1	<.1	<.1	<.1	<.1	<.1
Co	2.7	2.3	2.1	2.7	1.7	1.1	<.5	0.7
Cs	0.5	0.9	0.5	0.7	0.7	0.6	0.5	0.9
Cu	0.4	0.7	1	12.8	0.6	0.8	0.5	0.6
Ga	14.4	15.2	15.2	13.2	14.2	17.4	16.5	19.4
Hf	4.9	4.6	4.2	5.4	3.8	3.3	2.6	2.9
Hg	<.01	<.01	<.01	<.01	<.01	<.01	<.01	<.01
Mo	0.2	0.2	0.2	0.3	1.5	0.3	0.4	0.4
Nb	8.4	8.1	9.1	9.7	7.9	8	9.1	7.5
Ni	0.8	0.8	1.2	1.3	1.4	0.7	0.6	0.8
Pb	3	3	2.1	5	2.8	10.6	5	7.8
Rb	77	101.4	125.3	88.9	100.2	148.2	142.1	117.2
Sb	<.1	0.1	<.1	<.1	<.1	<.1	<.1	<.1
Sc	6	3	5	7	3	3	2	2
Se	<.5	<.5	<.5	<.5	<.5	<.5	<.5	<.5
Sn	1	2	1	2	2	2	<1	1
Sr	100.7	109.9	136.8	75.6	96.9	108.5	103.2	119.6
Ta	0.3	0.7	0.5	0.7	0.7	0.7	0.6	0.3
Tl	<.1	<.1	<.1	<.1	0.2	<.1	<.1	<.1
Th	14	18.6	35	16.8	18.2	11.1	8.1	10.1
U	3.7	3.2	2.9	3.7	8.5	14.6	11.6	18.3
V	10	20	17	15	10	13	6	<5
W	1.5	0.6	1.4	1.3	0.7	2.3	0.3	0.4
Zr	161.8	137.3	127	165.6	122.9	73.5	56.4	63.9
Y	14.7	20.8	18.7	24.7	46.7	10.5	14.7	12.3
Zn	25	21	46	25	15	23	12	24
Au ppb	1.9	3	2.6	3.2	2.2	2.7	2.3	1.9

Sample	KFM08B 91.36A	KFM01B 36.66	KFM01B 41.89	KFM01B 416.5	KFM02A 483.64	KFM02A 495.64	KFM02A 502.64	KFM02A 503.78
Sample type	**Fresh**	**Altered**	**Altered**	**Altered**	**Altered**	**Altered**	**Altered**	**Altered**
La ppm	28.6	47.3	30.2	33.6	34.4	23.9	14.1	19.5
Ce	59.4	94.7	78.1	64	72.8	46.5	27.5	37.8
Pr	6.09	9.14	7.36	6.71	7.2	4.61	2.78	3.81
Nd	22.7	29.4	25	22.9	23.9	15.3	9.4	12.3
Sm	4	5.6	5.1	4.6	4.6	2.6	1.8	2.4
Eu	0.49	0.62	0.54	0.47	0.58	0.61	0.47	0.45
Gd	3.31	4.39	3.99	4.31	5.1	2.16	1.81	2.06
Tb	0.53	0.72	0.75	0.72	0.94	0.32	0.36	0.34
Dy	2.74	3.8	3.9	4.44	6.16	1.98	2.2	1.82
Ho	0.55	0.77	0.72	0.83	1.41	0.37	0.49	0.38
Er	1.39	1.78	1.77	2.37	4.84	1.05	1.53	1.15
Tm	0.19	0.29	0.29	0.4	0.77	0.17	0.29	0.21
Yb	1.18	1.44	1.52	2.03	5	0.9	1.86	1.17
Lu	0.17	0.26	0.23	0.38	0.85	0.14	0.23	0.22

Sample	KFM02A 506.8	KFM05A 691.58	KFM07A 183.13R	KFM08A 623.13R	KFM08B 91.36R
Sample type	**Altered**	**Altered**	**Altered**	**Altered**	**Altered**
Rock code	101057	101057	101057	101057	101057
SiO_2 wt%	74.19	68.24	74.32	74	73.47
Al_2O_3	13.17	15.35	12.74	12.64	13.17
Fe_2O_3	2.24	3.7	2.01	2.81	2.43
MgO	0.55	1.04	0.34	0.4	0.38
CaO	1.29	3.56	1.24	1.34	1.02
Na_2O	3.66	4.6	4.05	4.46	4.27
K_2O	3.77	1.84	3.95	2.92	3.98
TiO_2	0.21	0.47	0.2	0.23	0.21
P_2O_5	0.07	0.21	0.05	0.06	0.06
MnO	0.04	0.05	0.03	0.03	0.04
Cr_2O_3	0.013	0.004	0.012	0.014	0.021
LOI	0.9	0.8	1	0.9	0.9
TOT/C	0.03	0.03	0.02	0.01	0.03
TOT/S	0.01	0.01	0.01	0.01	0.01
SUM	100.1	99.87	99.94	99.8	99.95
S ppm	n.a.	n.a.	63.8	10.8	37.8
Ag	<.1	<.1	<.1	<.1	<.1
As	<.5	<.5	<.5	<.5	<.5
Ba	1,066	1,262.1	1,240	1,797	1,149.4
Be	2	2	2	2	2
Bi	<.1	0.1	<.1	<.1	<.1
Cd	<.1	0.1	<.1	0.1	<.1
Co	2.7	7.6	2.5	2.9	2.6
Cs	1.2	1	0.5	0.2	0.3
Cu	0.6	33.7	1.7	0.7	1.1
Ga	16.3	21.8	13	13.8	13.5
Hf	5.8	5.5	3.9	5.9	4.8
Hg	<.01	<.01	<.01	<.01	<.01
Mo	0.3	0.8	0.4	0.3	0.3
Nb	12.6	11	9.4	13.5	7.9
Ni	1.4	6.7	1.1	1.1	1.4
Pb	2.9	3	4.1	6	4.8
Rb	100.9	78.5	103.3	64.9	100.3
Sb	<.1	<.1	<.1	<.1	<.1
Sc	5	4	5	6	6
Se	<.5	<.5	<.5	<.5	<.5
Sn	2	3	2	4	<1
Sr	110.2	924.6	80.4	103.6	69.7
Ta	0.8	1.3	0.5	2.1	0.3
Tl	<.1	0.3	<.1	<.1	<.1
Th	16.7	10.7	15.5	17	16
U	5.9	2.3	3.7	4.2	3
V	10	39	8	13	12
W	1	10.1	0.6	1	0.6
Zr	176.6	194.7	136.1	201.6	178.4
Y	26.2	20.2	28.4	47.3	15.4
Zn	29	52	19	18	27
Au ppb	2.9	2.8	2.3	12.1	2

Sample	KFM02A 506.8	KFM05A 691.58	KFM07A 183.13R	KFM08A 623.13R	KFM08B 91.36R
Sample type	**Altered**	**Altered**	**Altered**	**Altered**	**Altered**
La ppm	37.9	54.7	46.9	51.7	42.5
Ce	79.9	112.5	95.5	101.2	88.7
Pr	7.95	11	9.27	10.05	8.49
Nd	28	34.9	32.6	38	29.8
Sm	5.2	4.6	5.7	6.3	6.1
Eu	0.68	1.09	0.65	0.73	0.54
Gd	5	3.13	4.62	5.66	4.01
Tb	0.91	0.46	0.71	1.07	0.61
Dy	4.76	2.84	4.8	6.61	3.23
Ho	0.95	0.53	0.89	1.51	0.5
Er	2.47	1.94	2.81	4.65	1.38
Tm	0.37	0.45	0.49	0.8	0.21
Yb	2.07	2.65	3.02	5.69	1
Lu	0.35	0.58	0.47	0.93	0.19

Appendix 3

SEM-EDS analyses of biotite and chlorite

Sample		Mineral	Na_2O	MgO	Al_2O_3	SiO_2	K_2O	CaO	TiO_2	MnO	FeO	Total
KFM01B	397.41A	Biotite	0.0	5.6	15.4	34.0	9.7	0.0	1.3	0.4	28.4	94.7
KFM01B	397.41B	Biotite	0.0	5.6	15.0	35.2	9.4	0.0	2.8	0.5	28.1	96.5
KFM01B	397.41C	Biotite	0.0	6.1	15.0	34.9	9.6	0.0	2.2	0.4	28.0	96.2
KFM02A	712.45A	Biotite	0.0	7.4	14.8	35.2	9.6	0.0	2.0	0.5	25.2	94.7
KFM02A	712.45B	Biotite	0.0	7.3	14.3	34.7	9.5	0.0	2.4	0.5	25.1	93.7
KFM02A	712.45C	Biotite	0.0	7.4	14.7	35.0	9.6	0.0	2.3	0.5	24.6	94.0
KFM02A	949.87A	Biotite	0.2	8.6	15.6	36.3	9.8	0.0	2.7	0.4	23.3	96.9
KFM02A	949.87B	Biotite	0.3	9.3	15.8	36.8	9.8	0.0	1.9	0.4	23.2	97.5
KFM02A	949.87C	Biotite	0.3	9.2	15.6	35.2	8.3	0.2	1.9	0.5	24.3	95.4
KFM02A	712.45D	Biotite	0.0	7.2	14.5	34.3	9.3	0.0	2.2	0.5	24.5	92.5
KFM08A	623.13A	Biotite	0.2	5.6	14.6	34.1	9.3	0.0	2.0	0.4	27.4	93.7
KFM01A	477.30A	Biotite	0.3	9.4	15.5	35.1	9.1	0.0	1.9	0.4	23.1	94.6
KFM01A	477.30B	Biotite	0.0	8.7	14.7	35.2	9.4	0.2	2.4	0.5	23.7	94.7
KFM01A	477.30C	Biotite	0.2	9.4	15.3	35.9	9.5	0.0	1.9	0.5	23.3	96.0
KFM01A	477.30D	Biotite	0.0	8.7	15.0	35.3	9.8	0.0	2.3	0.4	23.2	94.6
KFM01A	477.30E	Biotite	0.2	9.0	15.2	35.8	9.6	0.0	2.2	0.5	23.0	95.5
KFM02A	521.27A	Biotite	0.2	7.9	15.2	35.9	9.6	0.1	2.1	0.5	25.0	96.4
KFM02A	521.27B	Biotite	0.2	7.5	14.6	35.1	9.6	0.0	2.6	0.4	24.7	94.6
KFM02A	521.27C	Biotite	0.0	8.2	14.5	35.5	9.7	0.0	1.7	0.7	24.8	95.1
KFM02A	521.27D	Biotite	0.3	8.1	14.6	35.5	9.5	0.2	1.9	0.6	24.9	95.6
KFM02A	953.25A	Biotite	0.3	7.5	15.2	36.3	9.9	0.0	2.1	0.7	24.7	96.7
KFM02A	953.25B	Biotite	0.0	7.7	15.2	35.3	9.9	0.0	2.2	0.7	24.9	95.9
KFM02A	953.25C	Biotite	0.0	7.6	16.1	35.8	9.6	0.0	2.4	0.6	24.2	96.2
KFM02A	495.64A	Chlorite	0.2	5.8	18.8	23.0	0.0	0.2	0.2	0.3	37.5	86.1
KFM02A	495.64B	Chlorite	0.2	5.3	16.1	27.6	0.7	1.5	2.5	0.5	32.8	87.3
KFM02A	502.64A	Chlorite	0.2	5.5	19.3	22.8	0.0	0.0	0.0	0.5	39.1	87.5
KFM02A	502.64B	Chlorite	0.2	7.6	18.5	24.4	0.0	0.0	0.0	0.4	36.7	87.8
KFM02A	506.80A	Chlorite	0.2	8.3	15.5	23.8	0.2	1.6	1.7	0.4	31.3	82.8
KFM02A	506.80B	Chlorite	0.0	8.9	18.9	23.7	0.0	0.0	0.0	0.3	34.7	86.5
KFM02A	506.80C	Chlorite	0.3	8.9	18.4	24.1	0.0	0.0	0.0	0.4	34.3	86.4
KFM02A	506.80D	Chlorite	0.3	9.0	18.9	24.1	0.0	0.0	0.0	0.2	34.1	86.6
KFM07A	183.13A	Chlorite	0.3	7.3	19.5	23.3	0.0	0.0	0.0	0.5	36.4	87.2
KFM07A	183.13B	Chlorite	0.3	6.6	16.7	26.4	0.2	1.3	1.7	0.4	35.2	88.7
KFM08B	91.36(O)A	Chlorite	0.2	6.4	15.5	24.4	0.0	0.2	0.2	0.4	36.7	84.0
KFM08B	91.36(O)B	Chlorite	0.3	6.8	15.5	24.5	0.0	0.5	0.5	0.4	35.7	84.1
KFM08B	91.36(O)C	Chlorite	0.4	7.3	15.3	25.6	0.1	0.5	0.8	0.4	35.0	85.4
KFM08B	91.36(R)A	Chlorite	0.3	6.4	16.4	26.6	0.0	1.8	1.8	0.5	37.5	91.3
KFM08B	91.36(R)B	Chlorite	0.4	6.6	16.8	25.9	0.0	0.2	0.0	0.5	39.6	90.0
KFM08B	91.36(R)C	Chlorite	0.4	7.5	16.7	26.7	0.0	0.3	0.3	0.4	39.4	91.6
KFM08A	623.13(R)	Chlorite	0.3	9.7	17.0	25.4	0.0	0.2	0.2	0.3	33.4	86.3

All values are in wt%.

Appendix 4

Modal analyses of thin sections

Sample type	KFM02A 712.45 Fresh	KFM02A 953.45 Fresh	KFM08B 91.36 O Fresh	KFM02A 949.87 Fresh	KFM01B 397.41 Fresh	KFM01A 521.27 Fresh	KFM01A 477.30 Fresh
Quartz (%)	38.1	32.9	41.7	40.2	46.4	35.7	54.0
Plagioclase	21.6	30.4	4.5	32.6	24.7	42.1	27.9
Sauss. Plag.	3.4	9.6	26.5	2.5	5.6	1.6	0.0
K-feldspar	31.9	22.6	20.9	17.1	16.6	8.8	9.0
Biotite	4.5	1.5	0.2	7.2	3.6	8.0	8.3
Epidote	0.5	1.1	0.7	0.2	2.0	3.6	0.8
Allanite	0.1	0.0	0.1	0.0	0.0	0.0	0.0
Opaque	0.0	0.9	0.3	0.2	0.5	0.2	0.0
Chlorite	0.0	0.5	5.2	0.1	0.5	0.0	0.0
Muskovite	0.0	0.6	0.0	0.0	0.0	0.0	0.0
Titanite	0.0	0.0	0.0	0.0	0.0	0.1	0.0
Amphibole	0.0	0.0	0.0	0.0	0.2	0.0	0.0
Calcite	0.0	0.0	0.0	0.0	0.0	0.0	0.0
Clay mineral	0.0	0.0	0.0	0.0	0.0	0.0	0.0
Pumpellyite	0.0	0.0	0.0	0.0	0.0	0.0	0.0

Sample type	KFM02A 495.64 Altered	KFM02A 506.80 Altered	KFM08B 91.36 R Altered	KFM02A 502.64 Altered	KFM07A 183.13R Altered	KFM01A 521.27 Altered	KFM08A 623.13R Altered	KFM02A 503.78 Altered
Quartz (%)	31.1	36.7	40.1	30.8	30.3	33.5	41.7	34.5
Plagioclase	2.4	2.2	0.3	0.0	0.0	0.0	0.0	0.0
Sauss. Plag.	28.8	38.6	37.4	33.7	41.7	36.9	40.5	36.7
K-feldspar	33.1	13.4	16.1	33.4	19.4	21.1	10.5	24.3
Biotite	0.0	0.0	0.0	0.0	0.0	0.0	0.0	0.0
Epidote	1.5	1.3	0.6	1.1	1.1	5.7	3.1	1.4
Allanite	0.0	0.3	0.0	0.0	0.0	0.0	0.0	0.4
Opaque	0.2	0.1	0.1	0.0	0.3	0.5	0.2	0.0
Chlorite	3.0	7.4	5.2	0.8	7.0	2.4	4.1	2.6
Muskovite	0.0	0.0	0.0	0.0	0.0	0.0	0.0	0.2
Titanite	0.0	0.1	0.1	0.0	0.0	0.0	0.0	0.0
Amphibole	0.0	0.0	0.0	0.0	0.0	0.0	0.0	0.0
Calcite	0.0	0.0	0.0	0.1	0.0	0.0	0.0	0.0
Clay mineral	0.0	0.0	0.0	0.1	0.3	0.0	0.0	0.0
Pumpellyite	0.0	0.0	0.1	0.1	0.0	0.0	0.0	0.0

Sauss. Plag. = Saussuritized plagioclase.